Ibi M Zou P Inoko A Shiromizu T Matsuyama M Hayashi Y Enomoto M Mori D Hirotsune S Kiyono T Tsukita S Goto H Inagaki M	Trichoplein controls microtubule anchoring at the centrosome by binding to Odf2 and ninein.	J Cell Sci.	124	857-64	2011
Kyo S Sakaguchi J Kiyono T Shimizu Y Maida Y Mizumoto Y Mori N Nakamura M Takakura M Miyake K Sakamoto M Inoue M.	Forkhead transcription factor FOXO1 is a direct target of progestin to inhibit endometrial epithelial cell growth.	Clin Cancer Res	17	525-37	2011
Mizumoto Y Kyo S Kiyono T Takakura M Nakamura M Maida Y Mori N Bono Y Sakurai H Inoue M.	Activation of NF-kB Is a Novel Target of KRAS-Induced Endometrial Carcinogenesis.	Clin Cancer Res	17	1341-50	2011
Miura S Kawana K Schust DJ Fujii T Yokoyama T Iwasawa Y Nagamatsu T Adachi K Tomio A Tomio K Kojima S Yasugi T Kozuma S Taketani Y	CD1d, a sentinel molecule bridging innate and adaptive immunity, is downregulated by the human papillomavirus (HPV) E5 protein: a possible mechanism for immune evasion by HPV.	J Virol	84	11614-23	2010

Adachi K Kawana K Yokoyama T Fujii T Tomio A Miura S Tomio K Kojima S Oda K Sewaki T Yasugi T Kozuma S Taketani Y	Oral immunization with Lactobacillus casei vaccine expressing human papillomavirus (HPV) type 16 E7 is an effective strategy to induce mucosal cytotoxic lymphocyte against HPV16 E7.	Vaccine	28	2810-7	2010
Yamashita H Okuma K Kawana K Nakagawa S Oda K Yano T Kobayashi S Wakui R Ohtomo K Nakagawa K	Comparison Between Conventional Surgery Plus Postoperative Adjuvant Radiotherapy and Concurrent Chemoradiation for FIGO Stage IIB Cervical Carcinoma: A Retrospective Study.	Am J Clin Oncol,	Epub	Epub	2010
Okuma K Yamashita H Kawana K Nakagawa S Oda K Nakagawa K	Advanced age is a significant determinant of poor prognosis in patients treated with surgery plus postoperative radiotherapy for endometrial cancer.	J Obstet Gynecol Res	36	757-763	2010
Shoji K Oda K Nakagawa S Kawana K Yasugi T Ikeda Y Takazawa Y Kozuma S Taketani Y	Aromatase inhibitor anastrozole as a second-line hormonal treatment to a recurrent low-grade endometrial stromal sarcoma: a case report.	Med Oncol	Epub	Epub	2010
Satsuka A Yoshida S Kajitani N Nakamura H Sakai H	A novel human papillomavirus type 18 replicon and its application in screening the anti-viral effects of cytokines	Cancer Sci.	101	536-42	2010
Ishii Y Tanaka K Kondo K Takeuchi T Mori S Kanda T	Inhibition of nuclear entry of HPV16 pseudovirus-packaged DNA by an anti-HPV16 L2 neutralizing antibody.	Virology	406	181-8	2010

Mori S Nakao S Kukimoto I Kusumoto-Matsuo R Kondo K Kanda T	Biased amplification of HPV DNA in specimens containing multiple HPV types by PCR with consensus primers.	Cancer Sci		in press	2011
Maeda D, Chen X, Guan B, Nakagawa S, Yano T, TaketaniY, Fukayama M, Wang TL, Shih IeM.	Rsf-1 (HBXAP) expression is associated with advanced stage and lymph node metastasis in ovarian clear cell carcinoma.	Int J Gynecol Pathol.	30	30-5	2011
Maeda D, Ota S, Takazawa Y, Ohashi K, Mori M, Imamura T, Nakagawa S, Yano T, Taketani Y, Fukayama M.	Mucosal carcinoma of the fallopian tube coexists with ovarian cancer of serous subtype only: a study of Japanese cases.	Virchows Arch	457	597-608	2010
Nagasaka K, Pim D, Massimi P, Thomas M, Tomaić V, Subbaiah VK, Kranjec C, Nakagawa S, Yano T, Taketani Y, Myers M, Banks L.	The cell polarity regulator hScrib controls ERK activation through a KIM site-dependent interaction.	Oncogene.	29	5311-21	2010
Hiraike H, Wada-Hiraike O, Nakagawa S, Koyama S, Miyamoto Y, Sone K, Tanikawa M, Tsuruga T, Nagasaka K, Matsumoto Y, Oda K, Shoji K, Fukuhara H, Saji S, Nakagawa K, Kato S, Yano T, Taketani Y.	Identification of DBC1 as a transcriptional repressor for BRCA1.	Br J Cancer.	29	1061-7	2010

Koyama S, Wada-Hiraike O, Nakagawa S, Tanikawa M, Hiraike H, Miyamoto Y, Sone K, Oda K, Fukuhara H, Nakagawa K, Kato S, Yano T, Taketani Y.	Repression of estrogen receptor beta function by putative tumor suppressor DBC1.	Biochem Biophys Res Commun.	392	357-62	2010
Murayama-Hosokawa S, Oda K, Nakagawa S, Ishikawa S, Yamamoto S, Shoji K, Ikeda Y, Uehara Y, Fukayama M, McCormick F, Yano T, Taketani Y, Aburatani H.	Genome-wide single-nucleotide polymorphism arrays in endometrial carcinomas associate extensive chromosomal instability with poor prognosis and unveil frequent chromosomal imbalances involved in the PI3-kinase pathway.	Oncogene	29	1897-908	2010
Endo S Yamato K Hirai S Moriwaki T Fukuda K Suzuki H Abei M Nakagawa I Hyodo I	Potent in vitro and in vivo antitumor effects of MDM2 inhibitor nutlin-3 in gastric cancer cells.	Cancer Sci	102	605-13	2011

Ⅳ　研究成果の刊行物・別冊

CDC6 interaction with ATR regulates activation of a replication checkpoint in higher eukaryotic cells

Kazumasa Yoshida, Nozomi Sugimoto, Satoko Iwahori, Takashi Yugawa, Mako Narisawa-Saito, Tohru Kiyono and Masatoshi Fujita*

Virology Division, National Cancer Center Research Institute, 5-1-1 Tsukiji, Chuohku, Tokyo 104-0045, Japan

*Author for correspondence (mafujita@ncc.go.jp)

Accepted 20 October 2009
Journal of Cell Science 123, 225-235 Published by The Company of Biologists 2010
doi:10.1242/jcs.058693

Summary

CDC6, a replication licensing protein, is partially exported to the cytoplasm in human cells through phosphorylation by Cdk during S phase, but a significant proportion remains in the nucleus. We report here that human CDC6 physically interacts with ATR, a crucial checkpoint kinase, in a manner that is stimulated by phosphorylation by Cdk. CDC6 silencing by siRNAs affected ATR-dependent inhibition of mitotic entry elicited by modest replication stress. Whereas a Cdk-phosphorylation-mimicking CDC6 mutant could rescue the checkpoint defect by CDC6 silencing, a phosphorylation-deficient mutant could not. Furthermore, we found that the CDC6-ATR interaction is conserved in *Xenopus*. We show that the presence of *Xenopus* CDC6 during S phase is essential for *Xenopus* ATR to bind to chromatin in response to replication inhibition. In addition, when human CDC6 amino acid fragment 180-220, which can bind to both human and *Xenopus* ATR, was added to *Xenopus* egg extracts after assembly of the pre-replication complex, *Xenopus* Chk1 phosphorylation was significantly reduced without lowering replication, probably through a sequestration of CDC6-mediated ATR-chromatin interaction. Thus, CDC6 might regulate replication-checkpoint activation through the interaction with ATR in higher eukaryotic cells.

Key words: CDC6, ATR, Cdk phosphorylation, Replication checkpoint, Higher eukaryotic cells

Introduction

In eukaryotic cells, chromosomal DNA replication is tightly regulated during the cell cycle and closely coordinated with other cell-cycle events, such as mitosis and DNA-damage response. The periodic assembly and disassembly of pre-replication complexes (pre-RCs) at replication origins is a central mechanism that ensures that there is only one DNA replication per single cell cycle (Bell and Dutta, 2002; Diffley, 2004; Fujita, 2006). During the period of low cyclin-dependent kinase (Cdk) from late mitosis through G1 phase, the origin recognition complex (ORC), CDC6 and Cdt1 load a presumptive replicative helicase, the MCM2-7 complex, onto chromatin to assemble the pre-RC. During the S, G2 and M phases, inappropriate reassembly of the pre-RC and subsequent re-replication are strictly prohibited by redundant suppression mechanisms against multiple MCM loaders. In human cells, Cdt1 activity is very tightly restricted by multiple pathways (Fujita, 2006). Human ORC1 is degraded through ubiquitylation by SCF^{Skp2} (Méndez et al., 2002). CDC6 is a target of Cdk and, although this leads to degradation in yeast (Drury et al., 1997; Jallepalli et al., 1997; Jallepalli et al., 1998; Kominami and Tada, 1997), the outcome in human cells is nuclear export (Fujita et al., 1999; Jiang et al., 1999; Petersen et al., 1999; Saha et al., 1998). Whereas phosphorylation of human CDC6 by Cdk negatively regulates its function in pre-RC formation (Sugimoto et al., 2009), it is noteworthy that a significant proportion of CDC6 proteins remains in the nuclei during S phase (Fujita et al., 1999), suggesting a potential CDC6 function(s) other than pre-RC assembly.

When chromosomal DNA is damaged, for example by DNA double-strand breaks (DSBs) and replication stress, cells activate DNA-damage response cascades to halt the cell cycle, repair the damage and, if necessary, induce apoptosis (Bartek and Lukas, 2003; Burrows and Elledge, 2008; Kastan and Bartek, 2004; Nyberg et al., 2002). Ataxia telangiectasia mutated (ATM) and ATM- and Rad3-related (ATR) kinases are phosphatidylinositol-3-kinase-related kinases and are major upstream kinases that signal several downstream pathways by phosphorylating many effector molecules, including the Chk1 and Chk2 kinases. The activated Chk1 and Chk2 eventually delay cell-cycle progression to facilitate DNA repair, mainly through inhibiting CDC25 phosphatases required for Cdk activation (Bartek and Lukas, 2003). ATM primarily responds to DSBs, and mainly phosphorylates and activates Chk2. Several other checkpoint factors co-function with ATM. For example, The Mre11-Rad50-Nbs1 complex is a sensor for DSBs, substrate for ATM and regulator of ATM activity (Lee and Paull, 2005).

ATR primarily responds to replication stress and mainly phosphorylates and activates Chk1 (Burrows and Elledge, 2008). A current model for ATR recruitment and activation at damaged sites is as follows: ATR forms a stable complex with the ATRIP (ATR-interacting protein; Cortez et al., 2001). When DNA replication is impeded, extensive single-stranded DNA (ssDNA) is generated through discordance between DNA polymerases and the MCM helicase, and then coated by replication protein A (RPA), which in turn recruits ATR through ATRIP binding (Namiki and Zou, 2006; Zou and Elledge, 2003). However, the need for the final step has been challenged by the recent identification of ATRIP mutants that are deficient in RPA binding and, thus, do not support stable ATR retention at damaged sites but still promote Chk1 phosphorylation (Ball et al., 2005; Kim et al., 2005). Also in this pathway, several crucial cofactors are required for optimal activation of ATR-Chk1. The Rad9-Rad1-Hus1 complex is a PCNA-like clamp loaded by Rad17-RFC onto damaged sites (Burrows and Elledge, 2008). TopBP1 promotes ATR kinase activity (Hashimoto et al., 2006; Kumagai et al., 2006), through interactions with Rad9-Rad1-Hus1 and ATR-ATRIP (Mordes et al., 2008). Claspin is a mediator that facilitates Chk1 phosphorylation by ATR (Lee et al., 2003).

Journal of Cell Science

Journal of Cell Science

However, the mechanisms for ATR recruitment and activation at damaged sites have yet to be completely elucidated.

Several studies in higher eukaryotic cells have implicated the CDC6 proteins in replication-checkpoint activation. In human cells, overexpression of CDC6 in G2 cells blocks mitotic entry by activating Chk1 (Clay-Farrace et al., 2003). In addition, Lau et al. showed that, despite CDC6 depletion in S-phase cells slowing replication, it does not activate Chk1 and leads to cells that prematurely enter mitosis with DNA synthesis (Lau et al., 2006). In an in vitro DNA-replication system with *Xenopus* egg extracts, *Xenopus* CDC6 (XCDC6) was shown to be required for XChk1 activation induced by replication inhibition (Oehlmann et al., 2004). Nevertheless, the molecular mechanism by which CDC6 contributes to replication-checkpoint activation remains unknown. Here, we show that human CDC6 physically interacts with ATR in a Cdk-phosphorylation-stimulated manner and that this interaction is required for proper activation of the replication checkpoint induced by modest replication stress. Further experiments suggested that a similar mechanism might also operate in *Xenopus* cells. In fission yeast, Cdc18 (CDC6) physically interacts with Rad3-Rad26 (ATR-ATRIP) via Rad26 to sustain the replication-checkpoint activation (Hermand and Nurse, 2007). Thus, involvement of CDC6/Cdc18 interaction with ATR-ATRIP in a replication checkpoint might be a conserved feature throughout eukaryotes.

Results

Human CDC6 physically interacts with ATR in a Cdk-phosphorylation-stimulated manner

We investigated whether human CDC6 physical interacts with certain checkpoint protein(s) by GST-CDC6 pulldown assays with HeLa cell nuclear extracts followed by immunoblotting. ATM and ATR, but not Chk1, Chk2, TopBP1, claspin, Nbs1 or Mre11, were pulled down specifically with GST-CDC6 (Fig. 1AII). Rad9-Hus1-Rad1 proteins also did not bind to GST-CDC6 (data not shown). In these assays, cyclin A and Cdh1, proteins that bind to CDC6 (Mailand and Diffley, 2005; Petersen et al., 1999), served as controls. To confirm whether endogenous proteins are associated with CDC6 in vivo, HeLa cell nuclear extracts were immunoprecipitated with an anti-CDC6 antibody. As shown in Fig. 1B, ATR co-precipitated with CDC6. Thus far, we have been unable to detect co-immunoprecipitation between endogenous CDC6 and ATM. Therefore, the CDC6-ATR interaction is considered to be physiologically important.

We then mapped the interaction domain(s) of CDC6 with ATR (Fig. 1C,D). GST-CDC6 and the truncated derivatives studied were mixed with HeLa cell nuclear extracts and bound proteins were analyzed. ATR was found to bind to CDC6 fragments (amino acids) 89-268 and 180-268, but the binding was significantly weaker with fragment 1-180 (Fig. 1D). Binding studies to further narrow the ATR-binding domain found that CDC6 180-220, which contains a Walker A motif of the AAA ATPase family (Fig. 1C) (Williams et al., 1997; Herbig et al., 1999), is sufficient for ATR interaction (Fig. 1D). As shown below, this fragment was also able to bind to *Xenopus* ATR. In these assays, cyclin A, which binds to CDC6 via the Cy motif, was retained with CDC6 1-180 and 89-268, but not with CDC6 180-268 and 180-220, as expected. ATR forms a complex with ATRIP (Cortez et al., 2001; Zou and Elledge, 2003). In the studies reported here, it was difficult to determine whether ATRIP is retained with full-length GST-CDC6 because our antibody against ATRIP (86 kDa) cross-reacted with GST-CDC6 (Fig. 1E). However, using truncated GST-CDC6 89-268 and 180-220, which could bind to ATR, we detected specific retention of ATRIP (Fig. 1E). Similar to ATR, there was only weak binding between ATRIP and GST-CDC6 1-180.

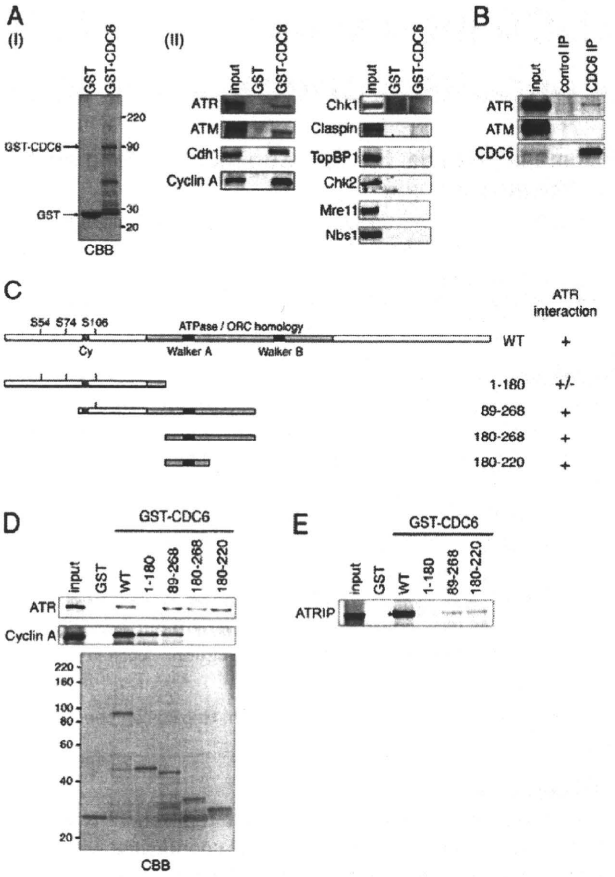

Fig. 1. Interaction of human CDC6 and ATR. (**A**) GST-CDC6 was incubated with HeLa cell nuclear extracts and bound proteins were analyzed by Coomassie Brilliant Blue (CBB) staining (I; left panel) or immunoblotting with the indicated antibodies (II; right panels). Fifteen percent of the input was also loaded. (**B**) HeLa cell nuclear extracts were immunoprecipitated with anti-CDC6 antibody or control rabbit IgG. The immunoprecipitates (IP) were subjected to immunoblotting. One percent of the input was also analyzed. (**C**) Schematic of wild-type human CDC6 and its truncated mutants used in D. The Cdk-phosphorylation sites (S54, S74, S106), cyclin-binding motif (Cy; R94 R95 L96) and ATPase/ORC-homology-domain containing Walker-A and -B motifs are marked. The ability of each mutant to interact with ATR, analyzed in D, is shown on the right. (**D**) Full-length GST-CDC6 (WT), its truncated mutants (amino acids 1-180, 89-268, 180-268 and 180-220) or GST were incubated with HeLa cell nuclear extracts and bound proteins were analyzed by CBB staining (lower panel) or immunoblotting. (**E**) Full-length GST-CDC6 (WT), its truncated mutants (1-180, 89-268 and 180-220) and GST were each incubated with HeLa cell nuclear extracts and bound proteins were immunoblotted with anti-ATRIP antibodies. The asterisk marks a non-specific band, with a molecular weight similar to ATRIP, due to cross-reaction of the anti-ATRIP antibody with GST-CDC6 WT.

When CDC6 is overexpressed in G2 cells, it blocks mitotic entry through Chk1 activation (Clay-Farrace et al., 2003). CDC6 has three Cdk-phosphorylation sites (S54, S74 and S106) (Jiang et al., 1999; Petersen et al., 1999) and Cdk phosphorylation is required for CDC6 activity to induce G2 arrest (Clay-Farrace et al., 2003). Therefore,

we investigated whether CDC6-ATR interaction might be regulated by Cdk phosphorylation. Wild-type CDC6, a phosphorylation-deficient CDC6 mutant (S54A, S74A, S106A) and a phosphorylation-mimic mutant (S54E, S74E, S106E) (Jiang et al., 1999) were tagged with tandem hemagglutinin (HA) at the N-terminus (2HA-CDC6 WT, AAA and EEE, respectively), and the vectors expressing CDC6 were transiently transfected into 293T cells. The nuclear extracts were then immunoprecipitated with anti-HA antibodies. ATR co-precipitated with 2HA-CDC6 WT and EEE, but little co-precipitated with the AAA mutant (Fig. 2A). However, the steady-state levels of 2HA-CDC6 AAA proteins and, therefore, the levels of immunoprecipitated AAA proteins were lower than 2HA-CDC6 WT and EEE upon transient expression (Fig. 2A), as expected from the fact that Cdk phosphorylation attenuates APC/C^{Cdh1}-mediated CDC6 degradation (Mailand and Diffley, 2005). Therefore, the amount of co-precipitated ATR was normalized to that of immunoprecipitated CDC6. These results demonstrated that the efficacy of ATR co-precipitation with 2HA-CDC6 AAA is reduced to ~40% compared with 2HA-CDC6 WT and EEE (Fig. 2A, lower panel). To demonstrate reciprocal co-immunoprecipitation, 293T cells were transfected with a vector expressing FLAG-ATR along with 2HA-CDC6 WT, AAA or EEE and immunoprecipitated with anti-FLAG antibodies (Fig. 2B). 2HA-CDC6 WT was co-precipitated specifically with FLAG-ATR. Immunoblotting with anti-phospho-S54-CDC6 antibodies revealed that CDC6 proteins phosphorylated by Cdk were co-precipitated. Although FLAG-ATR was precipitated with comparable efficacy in all experiments, the efficacy of 2HA-CDC6 AAA co-precipitation relative to the input was decreased to one-third that of the WT and, conversely, that of 2HA-CDC6 EEE increased threefold.

We studied this result further with a different system. 293T cells transiently expressing 2HA-CDC6 were treated with 10 mM purvalanol A, a specific inhibitor of Cdk1 and Cdk2 (Gray et al., 1998; Villerbu et al., 2002), or left untreated, and then immunoprecipitated with anti-HA antibodies. Also, in these experiments, the steady-state levels of 2HA-CDC6 were reduced by Cdk inhibition (Fig. 2C). Therefore, the amount of co-precipitated ATR was normalized to that of immunoprecipitated 2HA-CDC6. The efficiency of ATR co-precipitation was found to be reduced to ~25% by purvalanol-A treatment (Fig. 2C, lower panel). Cells were also treated simultaneously with purvalanol A and MG132, an inhibitor of 26S proteasomes, and immunoprecipitated with anti-HA antibodies. Simultaneous MG132 treatment decreased the reduction in 2HA-CDC6 by Cdk inhibition (Fig. 2C). Even under

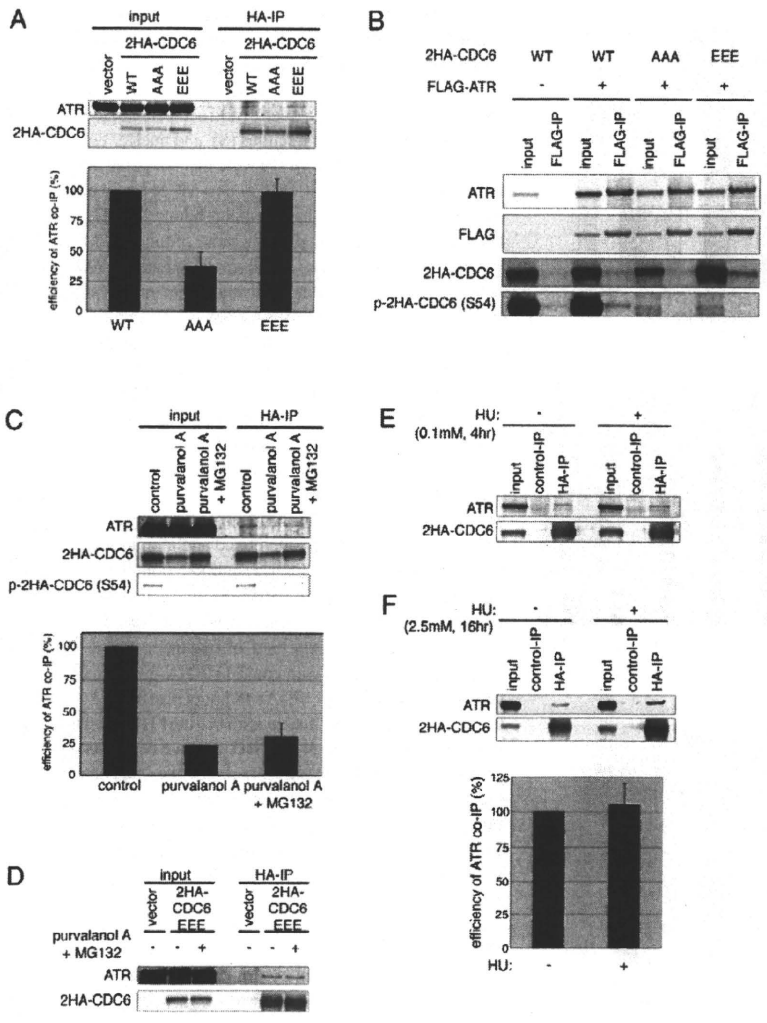

Fig. 2. Stimulation of CDC6-ATR interaction by Cdk phosphorylation. **(A)** 293T cells were transfected with expression vectors for 2HA-CDC6 wild type (WT), the AAA mutant (S54A, S74A, S106A), the phospho-mimic EEE mutant (S54E, S74E, S106E) or with a control vector and then immunoprecipitated with anti-HA antibody at 48 hours post-transfection. The immunoprecipitates (IP) and 1% of the inputs were immunoblotted with anti-CDC6 and anti-ATR antibodies. The signal intensities of the bands were quantitated and the efficiency of ATR co-immunoprecipitation (ATR co-IP) was calculated as the intensity of the co-precipitated ATR relative to that of the precipitated CDC6. The mean ± s.d. from three independent experiments are given with the WT value set at 100% (lower panel). **(B)** 293T cells were transfected with expression vectors for 2HA-CDC6 WT, AAA or EEE, along with an expression vector for FLAG-ATR or a control vector and then immunoprecipitated with anti-FLAG antibodies at 48 hours post-transfection. The immunoprecipitates (IP) and 4% of the inputs were immunoblotted with the indicated antibodies. **(C)** 2HA-CDC6 (WT) was transiently expressed in 293T cells and immunoprecipitated 48 hours post-transfection. As indicated, 10 μM purvalanol A, an inhibitor of Cdk1 and Cdk2, was added to the medium, with or without 20 μM MG132, at 3 hours before harvest. The precipitates and 1% of the inputs for ATR or 20% of the input for 2HA-CDC6 were immunoblotted. The efficiency of ATR co-IP was calculated as described in A and the mean ± s.d. from two independent experiments are given with the control value set at 100% (lower panel). **(D)** The same experiments as in C were carried out with 2HA-CDC6 EEE. **(E,F)** HU treatment at 0.1 mM for 4 hours (E) or 2.5 mM for 16 hours (F) does not alter the CDC6-ATR interaction. 293T cells were transfected with the vector for 2HA-CDC6 WT and then treated with HU as above before harvest or left untreated. At 48 hours post-transfection, cells were subjected to immunoprecipitation with anti-HA antibodies as described in A. For the experiments shown in F, incubation with 2.5 mM HU for 16 hours arrested most cells in S phase, leading to CDC6 accumulation. Therefore, the amount of co-precipitated ATR was normalized to that of immunoprecipitated 2HA-CDC6, as in A, and the mean ± s.d. from two independent experiments are given with the value of untreated cells set at 100% (lower panel).

such conditions, the efficacy of ATR co-precipitation decreased to ~30% by purvalanol-A treatment (Fig. 2C). Immunoblotting with anti-phospho-S54-CDC6 antibodies revealed that purvalanol-A treatment indeed inhibited phosphorylation of 2HA-CDC6 by Cdk (Fig. 2C). In addition, we found that the interaction between ATR and 2HA-CDC6 EEE was not affected by purvalanol-A treatment (Fig. 2D), further supporting the notion that this drug affects ATR-CDC6 through inhibition of CDC6 phosphorylation by Cdk.

Taken together, these data led us to conclude that interaction of ATR with CDC6 is enhanced by CDC6 phosphorylation by Cdk. When cells are synchronized in early-mid G1 phase (6 hours after release from nocodazole arrest), CDC6 protein levels are remarkably decreased by APC/C^{Cdh1}-mediated ubiquitylation (data not shown) (Méndez and Stillman, 2000; Mailand and Diffley, 2005). As a result, in the present study, CDC6 immunoprecipitation with anti-CDC6 antibodies was remarkably reduced and ATR co-precipitation was undetectable in such cells (data not shown). Therefore, the observed co-precipitation between CDC6 and ATR in asynchronous cells might mainly represent interactions in S-phase cells. When cells were treated with 0.1 mM hydroxyurea (HU) for 4 hours, a condition we used to investigate CDC6 involvement in replication-checkpoint activation (see below), co-precipitation of ATR with CDC6 was not enhanced (Fig. 2E). Even with 2.5 mM HU treatment for 16 hours, the efficacy of the interaction was not changed (Fig. 2F).

CDC6 depletion by siRNA impairs ATR-dependent replication-checkpoint response and the defect is rescued by the CDC6 EEE mutant but not by CDC6 AAA

To determine whether CDC6 depletion by siRNA affects activation of a replication checkpoint in human cells, we designed siRNAs targeting 5′ untranslated regions of *CDC6* mRNA. Treatment with the *CDC6* siRNAs (6 nM) for 48 hours reduced the level of total CDC6 proteins to ~30% in HeLa cells compared with control-siRNA-treated cells (Fig. 3A). The effect was specific, because the level of MCM7 was not affected. Subcellular fractionation experiments showed that the level of chromatin-bound MCM7 proteins was decreased to ~70% by CDC6 depletion (Fig. 3A). Fluorescence-activated cell-sorting analysis showed that the cell-cycle distribution pattern is only slightly affected by CDC6 depletion (Fig. 3B). Cell growth was also largely unaffected (data not shown). Under the present experimental conditions in HeLa cells, CDC6 depletion did not induce spontaneous Chk1 phosphorylation (Fig. 3C), as reported previously (Lau et al., 2006; Kan et al., 2008). By

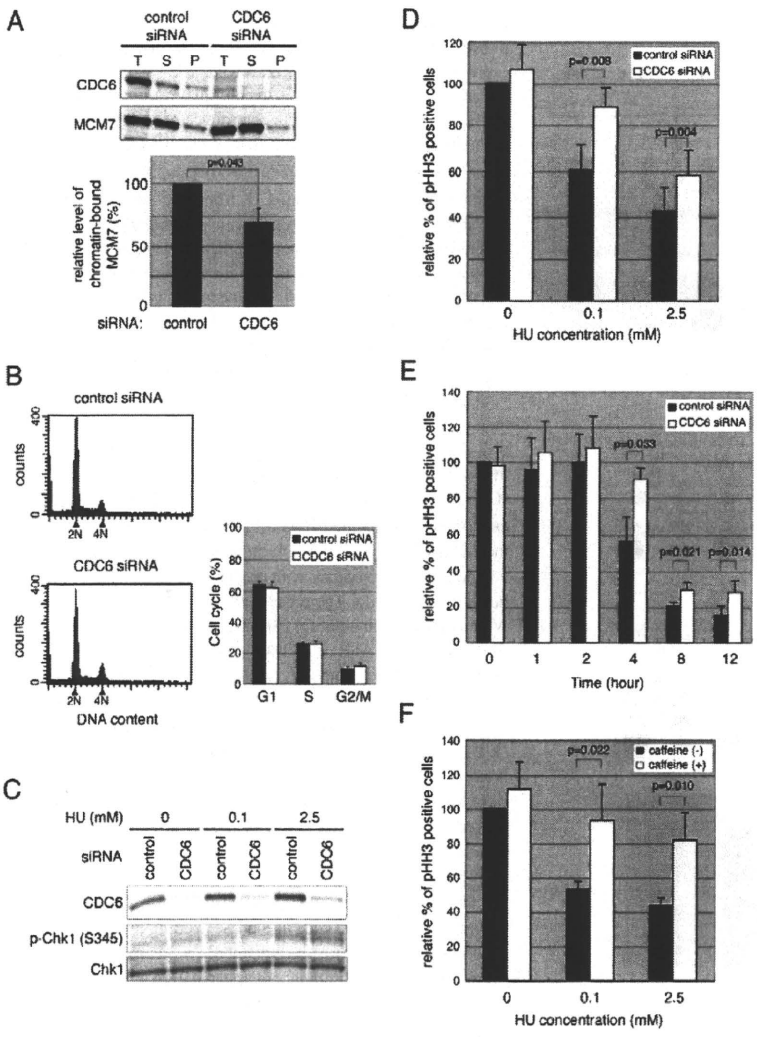

Fig. 3. CDC6 depletion by siRNA impairs the ATR-dependent replication-checkpoint response activated by modest replication stress. HeLa cells were transfected with siRNAs targeting 5′ untranslated regions of *CDC6* mRNA or with control siRNA for 48 hours. (**A**) Total cell extracts (T), Triton-X-100-extractable fractions (S), and nuclear chromatin and nuclear-matrix fractions (P) were then prepared and immunoblotted with anti-CDC6 or anti-MCM7 antibodies. The signal intensities of the chromatin-bound MCM7 proteins were quantified and normalized to those of total MCM7 to calculate the relative levels of chromatin-bound MCM7. The mean ± s.d. from three independent experiments are shown with the value for control-siRNA-treated cells set at 100 (lower panel). (**B**) Cell-cycle profiles were also analyzed by flow cytometry. The mean ± s.d. from three independent experiments are shown (right panel). (**C**) At 48 hours post-siRNA transfection, cells were treated with 2.5 mM or 0.1 mM HU, or left untreated, for a further 4 hours. Whole-cell lysates were then subjected to immunoblotting. p-Chk1, phospho-Chk1. (**D**) At 48 hours post-siRNA transfection, cells were treated with 2.5 mM or 0.1 mM HU, or left untreated, for a further 4 hours. Cells were then fixed and immunostained with anti-phospho-histone-H3 (pHH3) antibody followed by DAPI staining. The percentage of pHH3-positive cells was determined by microscopic observation of at least 3000 cells for each sample. The mean ± s.d. of five independent experiments are shown with control-siRNA-treated cells without HU set at 100%. (**E**) At 48 hours post-siRNA transfection, cells were treated with 0.1 mM HU for the times indicated. The percentage of pHH3-positive cells was then determined as in D. The mean ± s.d. of three independent experiments are shown with control-siRNA-treated cells at time 0 set at 100%. (**F**) At 48 hours after transfection with control siRNA, cells were incubated with 2.5 mM or 0.1 mM HU, or left untreated, for a further 4 hours. During the last 10 hours of incubation (i.e. from 6 hours before HU addition), 5 mM caffeine was also added, as indicated. The percentage of pHH3-positive cells was then determined as in D. The mean ± s.d. from four independent experiments are given with the value for control cells without drugs set at 100%.

Journal of Cell Science

contrast, it was reported that, when CDC6 is further depleted with more siRNAs (~100 nM), MCM loading is further reduced, leading to cell-cycle arrest around G1-S and/or cell death (Feng et al., 2003; Lau et al., 2009). Under such conditions, spontaneous Chk1 phosphorylation is observed.

We then investigated whether CDC6 depletion impairs ATR-mediated Chk1 phosphorylation induced by replication stress, such as polymerase inhibition. For these studies, CDC6-depleted or control-siRNA-treated HeLa cells were further treated with 2.5 mM HU for 4 hours and Chk1 phosphorylation was monitored with anti-phospho-S345-Chk1 antibodies (Zhao and Piwnica-Worms, 2001). As shown in Fig. 3C, robust phosphorylation of Chk1 was induced by 2.5 mM HU treatment and was not affected by CDC6 depletion, in agreement with previous findings that CDC6 depletion does not abolish Chk1 phosphorylation induced by treatment with 5 μg aphidicolin/ml in HeLa cells (Lau et al., 2006). Given the report that Chk1 phosphorylation induced by 1.5 mM HU treatment in HeLa cells is suppressed by 5 mM caffeine (Rodríguez-Bravo et al., 2006), an inhibitor for ATM and ATR, the above data and that of Lau et al. (Lau et al., 2006) suggest that CDC6 does not play a pivotal role in ATR activation by the stalled forks generated by 2.5 mM HU or 5 μg aphidicolin/ml.

However, Lau at el. also reported that CDC6-depleted HeLa cells (not treated with any drugs) prematurely enter mitosis despite the existence of actively replicating DNA (Lau et al., 2006). This suggested to us that CDC6 might be involved in replication-checkpoint activation elicited by modest replication stress. Extensive RPA-coated ssDNA is currently considered to be a crucial intermediate for ATR activation (Burrows and Elledge, 2008; Namiki and Zou, 2006; Zou and Elledge, 2003). We hypothesized that, although CDC6 is not necessarily required for activation of a replication checkpoint when there is sufficient RPA-coated ssDNAs, CDC6 might be required when replication stress is relatively modest. Therefore, because one crucial response elicited by replication-checkpoint activation involves a mitotic block (Kelly and Brown, 2000), we treated control-siRNA-transfected HeLa cells with various concentrations of HU for a relatively short period (i.e. 4 hours) and examined the effect of this on mitosis block by immunostaining the cells for phosphorylation of histone H3 at S10, a mitotic marker (data not shown). As expected, 2.5 mM HU treatment reduced the mitotic index to ~40% of that of untreated cells. Interestingly, we found that, even with 0.1 mM HU treatment, which reduces DNA synthesis by about 50% (Ge et al., 2007), HeLa cells were significantly inhibited in mitotic entry to a mitotic index of ~60%, suggesting that the replication checkpoint might be activated by low-dose HU treatment. We then tested whether CDC6 depletion affects the mitosis block. Although CDC6 depletion seemed to abrogate the mitotic block, at least partially, at all the HU concentrations tested, the effect was most prominent when cells were treated with 0.1 mM HU (data not shown). Therefore, we examined in more depth the influence of CDC6 depletion on mitotic block elicited by a 4-hour 0.1 mM HU treatment. As shown in Fig. 3D, CDC6 depletion increased the percentage of phospho-histone H3 (pHH3)-positive, mitotic cells by ~30% in cells treated with 0.1 mM HU, whereas it increased mitotic cells by only ~15% on treatment with 2.5 mM HU, suggesting that CDC6 plays a crucial role in replication-checkpoint activation by modest replication stress. Furthermore, we examined the effect of CDC6 depletion on mitotic block induced by 0.1 mM HU treatments at various time points (Fig. 3E). Longer incubation (8 and 12 hours) in the presence of 0.1 mM HU further decreased the amount of mitotic cells. Also under such conditions, CDC6 depletion resulted in a statistically significant increase in mitotic cells (Fig. 3E). However, the extent seemed to be limited compared with the 4-hour incubation.

Although the ATR-Chk1 pathway is a major component in replication-checkpoint activation (Guo et al., 2000; Hekmat-Nejad et al., 2000; Kumagai et al., 1998; Nghiem et al., 2001), several previous studies have indicated the existence of another pathway(s) to prevent premature mitotic entry upon replication stress (Brown and Baltimore, 2003; Rodríguez-Bravo et al., 2006; Zachos et al., 2003; Zachos et al., 2005). For example, it was previously shown that inhibition of mitotic entry in HeLa cells caused by 1.5 mM HU treatment for 25 hours is dependent on Chk1 and claspin but not on ATR and Rad17 (Rodríguez-Bravo et al., 2006). Therefore, we examined whether the replication-checkpoint response elicited by 0.1 mM (or 2.5 mM) HU for 4 hours depends on ATR by co-treating cells with HU and 5 mM caffeine. In order to compare the effect of caffeine with CDC6 depletion that occurs before the HU treatment (data not shown), we treated cells with 5 mM caffeine from 6 hours before the addition of HU. Caffeine was able to overcome the inhibition of mitotic entry induced by 0.1 mM HU (Fig. 3F), suggesting that activation of the replication checkpoint elicited by these experimental conditions depends on ATR (or possibly ATM). We found no detectable increase in Chk1 phosphorylation at S345 upon treatment with 0.1 mM HU for 4 hours (Fig. 3C). Therefore, even by modest replication stress in which Chk1 phosphorylation is not increased to an experimentally detectable level, an ATR-dependent replication checkpoint is activated and elicits a G2 arrest. This seems consistent with the fact that, in *Xenopus* egg extracts, ATR is required to prevent premature mitotic entry not only when replication is inhibited by exogenous stress but also during normal DNA replication, which might generate some internal replication stress (Hekmat-Nejad et al., 2000). Caffeine increased mitotic cells by ~40% also with 2.5 mM HU treatment (Fig. 3F) and the extent of recovery was higher than with CDC6 depletion (Fig. 3D), suggesting that CDC6 has rather a minor role in replication-checkpoint activation by strong replication stress.

To determine whether the abrogation of the checkpoint response is specifically due to the CDC6 depletion, we performed 'add-back' experiments. Because CDC6 interaction with ATR is enhanced by Cdk phosphorylation, we compared CDC6 EEE and CDC6 AAA. We established HeLa cell lines stably expressing 2HA-CDC6 AAA or EEE at similar levels (Fig. 4A). Analysis for subcellular localization of 2HA-CDC6 showed that almost all CDC6 AAA is bound to the chromatin and nuclear matrix, whereas most CDC6 EEE is in the soluble fraction with the rest bound to the chromatin and nuclear matrix (Sugimoto et al., 2009). These cells were then transfected with siRNAs targeting 5′ untranslated regions of *CDC6* mRNA, or control siRNA. Immunoblot analysis showed that exogenous 2HA-CDC6 protein levels were not affected by *CDC6* siRNA, whereas endogenous CDC6 decreased to ~30% (Fig. 4A).

Cells were further treated with 0.1 mM HU for 4 hours and mitotic indexes were determined. It has been reported that ionizing-radiation-induced DSBs activate the DNA-damage checkpoint, lead to Cdk downregulation and consequently induce APC/C^{Cdh1}-mediated CDC6 degradation (Duursma and Agami, 2005; Mailand and Diffley, 2005). CDC6 is also destabilized upon ultraviolet radiation (UV) and methyl-methane-sulfonate treatment through Huwe1-mediated ubiquitylation (Hall et al., 2007). We therefore examined the effects of HU treatment on CDC6 stability. The levels of endogenous CDC6 proteins in HeLa cells were not affected by

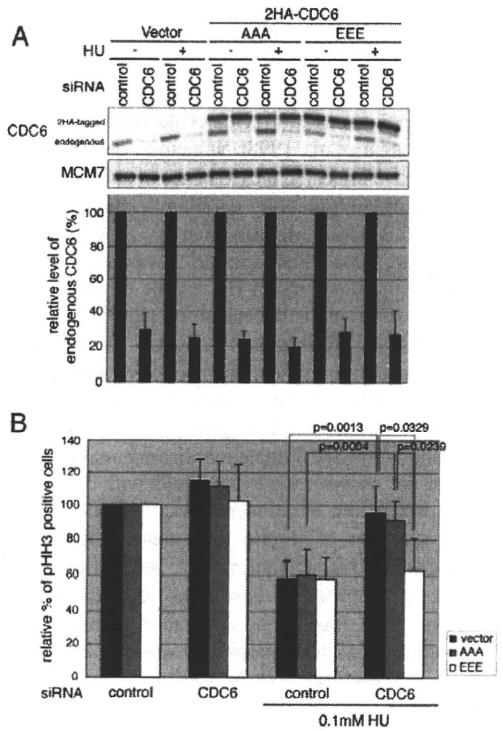

Fig. 4. The Cdk-phosphorylation-mimic CDC6 EEE mutant, but not the phospho-deficient AAA mutant, can rescue the defect in the replication-checkpoint response caused by CDC6 depletion. HeLa cells stably expressing the 2HA-CDC6 AAA or EEE mutant, or carrying a backbone vector, were established by retroviral infection. These cells were transfected with siRNAs targeting 5′ untranslated regions of *CDC6* mRNA or control siRNA for 48 hours, as described for Fig. 3. At 48 hours post-siRNA-transfection, cells were treated with 0.1 mM HU or left untreated for a further 4 hours. (**A**) Whole-cell lysates were immunoblotted. The signal intensities of the endogenous CDC6 bands were quantified and normalized to those of MCM7 to calculate CDC6 depletion efficiencies in each experiment. The mean ± s.d. from five independent experiments are shown with the value for control-siRNA-treated cells set at 100 (lower panel). (**B**) Cells were stained for pHH3 to determine the percentage of pHH3-positive cells, as described for Fig. 3. The mean ± s.d. of five independent experiments are shown with control-siRNA-treated cells without HU set at 100%.

either 0.1 mM or 2.5 mM HU treatment for 4 hours (Fig. 3C, Fig. 4A). Furthermore, the stability of transfected CDC6 AAA and CDC6 EEE mutant proteins was not differentially affected in response to 0.1 mM HU treatment for 4 hours (Fig. 4A). We also found that CDC6 is not destabilized by an 18-hour 2.5 mM HU treatment in normal human fibroblasts (data not shown). As reported, 10 or 25 J/m^2 UV irradiation resulted in CDC6 destabilization (data not shown). Therefore, replication-checkpoint activation by HU treatment might inhibit Cdk activity only to the extent that is insufficient for mitotic entry but enough for S-phase maintenance. It is generally considered that mitotic entry requires high Cdk activity.

In control HeLa cells with the backbone vector, CDC6 depletion abrogated the checkpoint response induced by 0.1 mM HU (Fig. 4B), as with parental HeLa cells. By contrast, despite *CDC6* siRNA treatment, mitotic entry was inhibited in HeLa cells with 2HA-CDC6 EEE (Fig. 4B), clearly demonstrating the CDC6 requirement for the ATR-dependent mitotic-block response. Interestingly, CDC6 AAA could not rescue the checkpoint defect (Fig. 4B). It was previously shown that *Xenopus* CDC6 mutants deficient in Cdk phosphorylation support normal replication with an efficiency comparable to that of wild type (Pelizon et al., 2000). We also found that 2HA-CDC6 AAA induces stronger re-replication than CDC6 EEE when transiently overexpressed with Cdt1 (Sugimoto et al., 2009). Therefore, CDC6 AAA might represent a novel mutant that specifically loses the ability to regulate ATR-dependent replication-checkpoint activation but retains the pre-RC-formation function. Taken together, these data strongly indicate that, in human cells, Cdk-phosphorylation-stimulated CDC6 interaction with ATR has a crucial role in replication-checkpoint activation elicited by modest replication stress.

The ATR-dependent checkpoint is also activated by UV irradiation. Thus, we tried to evaluate the role of CDC6 in UV-induced checkpoint activation. HeLa cells were irradiated with various doses of UV and, after 4 hours, examined for mitotic block and Chk1 phosphorylation. UV irradiation blocked mitotic entry in a dose-dependent manner, and Chk1 phosphorylation was also observed in a dose-dependent manner (data not shown). We then investigated the effects of CDC6 depletion on such UV-activated checkpoint responses. In contrast to HU treatment, CDC6-depleted HeLa cells were inhibited from mitotic entry in response to UV irradiation with comparable efficiency to control-siRNA-treated cells. Likewise, Chk1 phosphorylation was not affected by CDC6 depletion (data not shown). These data suggest that CDC6 might not be involved in UV-induced checkpoint responses. It is possible that intermediates for checkpoint activation and subsequent signaling pathways are different in some aspects between nucleotide-depletion-induced and UV-induced damage. For example, although 25 J/m^2 UV induced Chk1 phosphorylation at a comparable level to that by 2.5 mM HU treatment for 4 hours, the former inhibited mitotic entry more strongly (~100% versus ~60% inhibition) and destabilized CDC6 (data not shown). Whereas 0.1 mM HU treatment for 4 hours induced an ~40% mitotic block without detectable Chk1 phosphorylation (Fig. 3C-F), 5 J/m^2 UV inhibited mitosis by only ~20% despite obvious Chk1 phosphorylation (data not shown). Further in-depth studies will be required to dissect the molecular mechanisms.

Although our data indicate that CDC6-ATR interaction plays a role in the appropriate regulation of replication-checkpoint activation in human cells, it remains unclear how such interaction is involved in ATR activation. To address this issue, we first examined the possibility that CDC6 enhances ATR kinase activity as does TopBP1. Human ATR was immunopurified and the kinase activity was measured using PHAS1 as substrate. As previously reported (Hashimoto et al., 2006; Kumagai et al., 2006), addition of *Xenopus* Cut5 (XCut5; TopBP1) significantly increased the ATR kinase activity. Under these experimental conditions, GST-CDC6 EEE did not enhance the kinase activity. Addition of GST-CDC6 EEE to the reactions containing XCut5 also did not further increase the activity. Similar results were obtained with wild-type CDC6 (data not shown).

In fission yeast, Cdc18 stabilizes Rad3-Rad26 (ATR-ATRIP)-chromatin binding through physical interaction with Rad26 (Hermand and Nurse, 2007). Therefore, we examined whether stable ATR-chromatin binding is affected by CDC6 depletion in HeLa cells by immunodetecting the formation of bright nuclear ATR foci that might represent high-level accumulation of ATR at sites of DNA damage (Ball et al., 2005). The number of cells with

Journal of Cell Science

bright ATR foci increased slightly with 0.1 mM HU treatment for 4 hours and increased significantly with 2.5 mM HU treatment. However, the increase in number of ATR foci was not changed much by CDC6 depletion, suggesting that CDC6 is dispensable for stable high-level accumulation of ATR at sites at which DNA is extensively damaged. Also, clear colocalization of ATR foci with CDC6 was not observed (data not shown). Recently, it has been suggested that stable high-level retention of ATR at damaged sites is not necessarily required for some checkpoint responses (Ball et al., 2005). Therefore, it is possible that, although CDC6-ATR interaction does not mediate stable ATR retention at damaged sites, it does regulate dynamic association between ATR and small lesions. In this regard, it might be of interest that the human RPA complex binds to GST-CDC6 in pulldown assays, through the CDC6 region 1-180, which does not have a major role in CDC6-ATR interaction (data not shown).

XCDC6-XATR interaction is conserved in *Xenopus* and a human CDC6 fragment 180-220 that binds to XATR reduces XChk1 activation

In an in vitro DNA-replication system with *Xenopus* egg extracts, XCDC6 is required for XChk1 phosphorylation induced by polymerase inhibition (Oehlmann et al., 2004). Therefore, because XCDC6-XATR interaction might be conserved and play a crucial role in replication-checkpoint activation in *Xenopus* cells, we examined whether XCDC6 binds to XATR by pulldown assays. *Xenopus* egg extracts were mixed with GST or GST-XCDC6 and bound proteins were analyzed. XATR was found to bind to GST-XCDC6, but not to GST (Fig. 5A). In addition, XATR was found to co-immunoprecipitate with XCDC6 from egg extracts (Fig. 5B). Unfortunately, so far we could not determine whether the XCDC6-XATR interaction is affected by Cdk, mainly because of difficulty in specifically immunoprecipitating S-phase chromatin-bound XCDC6 with our anti-XCDC6 antibodies. Because CDC6-ATR interaction might be important for checkpoint activation, short CDC6 fragments that bind to XATR could inhibit XATR-dependent checkpoint responses by preventing physiological XCDC6-XATR interaction. Therefore, we repeated the pull-down experiments using *Xenopus* egg extracts and human CDC6 fragments fused to GST. As shown in Fig. 5C, XATR specifically bound to GST–human-CDC6. More importantly, XATR, similar to human ATR, bound to human CDC6 180-220 but not to CDC6 1-180 (Fig. 5C). The amino acid sequence of fragment 180-220 is conserved in XCDC6 (61% in identity). Taken together, these results indicate that CDC6-ATR interaction is a conserved feature in higher eukaryotic cells.

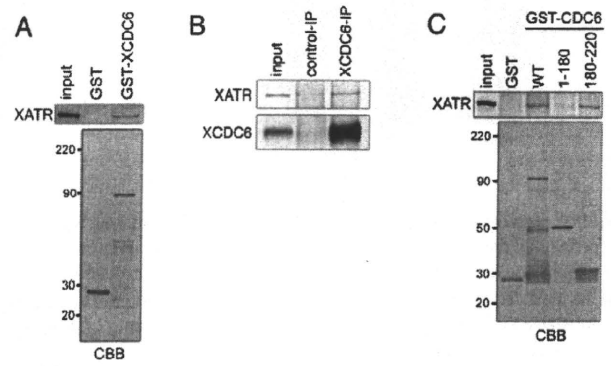

Fig. 5. CDC6-ATR interaction is conserved in *Xenopus* egg extracts. (**A**) GST–*Xenopus*-CDC6 (XCDC6) or GST was incubated with *Xenopus* egg extracts and bound proteins were analyzed by Coomassie Brilliant Blue (CBB) staining and immunoblotting with anti-XATR antibody. Fifty percent of the input was also loaded. (**B**) *Xenopus* egg extracts were immunoprecipitated with anti-XCDC6 antibodies or control rabbit IgG. The immunoprecipitates (IP) were subjected to immunoblotting with anti-XCDC6 and anti-XATR antibodies. A total of 1.6% of the input was also analyzed. (**C**) GST–human-CDC6 (WT; wild type), its truncated mutants (amino acids 1-180 and 180-220; see also Fig. 1) or GST was incubated with the egg extracts and bound proteins were analyzed by CBB staining and immunoblotting.

We first examined whether XCDC6 immunodepletion during S phase affects XATR recruitment onto chromatin in response to polymerase inhibition (Hekmat-Nejad et al., 2000). To address this, we adapted the nuclear transfer experiments (Fig. 6A). Licensed chromatin was isolated under high-salt conditions to remove chromatin-bound XCDC6 and then transferred to mock- or XCDC6-depleted extracts supplemented with aphidicolin to block DNA polymerases. After incubation for a further 45 minutes, chromatin was isolated and chromatin binding of XATR was analyzed by immunoblotting. Aphidicolin-induced recruitment of ATR to chromatin was significantly compromised by XCDC6 depletion (Fig. 6A). As previously reported (Oehlmann et al., 2004), DNA synthesis was not impaired by XCDC6 depletion from the second extracts (data not shown).

We found that the human CDC6 fragment 180-220 can partially prevent XATR binding to GST-XCDC6 when added to the egg extracts (Fig. 6B). Therefore, we tested whether this human CDC6 fragment can inhibit replication-checkpoint activation (Fig. 6C). For these studies, sperm chromatin was added to the egg extracts, which were then incubated for 15 minutes to allow pre-RC formation. Purified CDC6 fragment 180-220 with the SV40 T-antigen nuclear localization signal was then added to the reaction mixture at 10 ng/μl. The molar amount of CDC6 fragment was adjusted to 20-30 times higher than that of endogenous XCDC6 (Coleman et al., 1996). Aphidicolin (4 μg/ml) was also added to each reaction mixture and, after 45 minutes, isolated nuclei were immunoblotted with anti-phospho-S344-XChk1 antibody. Compared with control reactions with buffer alone or CDC6 fragment 1-180, which does not bind to XATR, phosphorylation of XChk1 induced by aphidicolin treatment was reduced by ~40% (Fig. 6D). We also investigated whether addition of CDC6 180-220 affects aphidicolin-induced recruitment of XATR to chromatin by immunoblotting analyses of chromatin fractions. Consistent with the reduction in XChk1 phosphorylation, aphidicolin-induced XATR chromatin recruitment was reduced by ~40% in the presence of CDC6 fragment 180-220 (Fig. 6E). In separate experiments, [^{32}P]-dCTP was added and the reactions were allowed to proceed for a further 45 minutes (without aphidicolin) after addition of the CDC6 fragments to monitor DNA replication. In all these reactions, DNA replication occurred at comparable levels (Fig. 6F), showing that the addition of CDC6 180-220 did not impair either pre-RC assembly or other replication reactions. Thus, human CDC6 fragment 180-220 specifically inhibits XATR-dependent XChk1 phosphorylation, probably through sequestrating XATR-XCDC6 interaction and XATR chromatin retention. Taken together, these data provide further support for our conclusion that CDC6 interacts with ATR and the CDC6-ATR interaction plays a crucial role in the regulation of replication-checkpoint activation in higher eukaryotic cells.

Journal of Cell Science

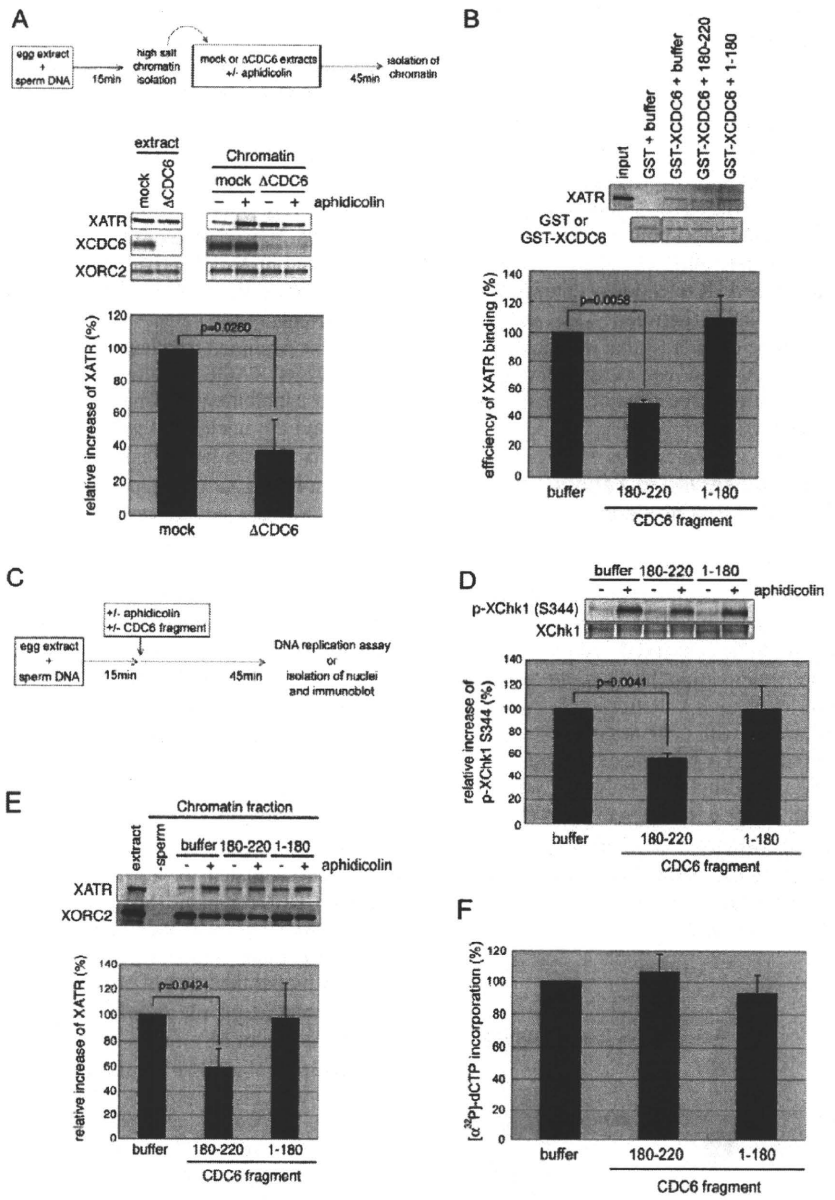

Fig. 6. CDC6-ATR interaction plays a role in activation of the replication checkpoint in *Xenopus* egg extracts. (A) XCDC6 immunodepletion during S phase reduces aphidicolin-induced XATR-chromatin binding. A schematic illustration of the experimental procedure is shown above. Sperm nuclei (4000/μl) were incubated in egg extracts for 15 minutes. Chromatin was then isolated under high-salt conditions and resuspended with mock- or XCDC6-depleted extracts. After a further 45-minute incubation, chromatin fractions were isolated and immunoblotted with the indicated antibodies. As indicated, aphidicolin (4 μg/ml) was added to the second extracts. The signal intensities of XATR bands induced by aphidicolin were normalized to those of XORC2 bands and plotted with the control reaction with mock-depleted extracts set at 100%. The mean ± s.d. from three independent experiments are shown. (**B-F**) Addition of human CDC6 amino acid fragment 180-220 after pre-RC assembly reduces XChk1 phosphorylation. (B) Human CDC6 fragments 180-220 or 1-180 with the SV40 T-antigen nuclear localization signal (but without GST) or buffer alone were added to *Xenopus* egg extracts. After incubation for 1.5 hours, these were then subjected to pulldown assays with GST-XCDC6, and bound proteins were analyzed by Coomassie Brilliant Blue (CBB) staining and immunoblotting. The signal intensities of the bands were quantitated and the efficiency of XATR binding to GST-XCDC6 was calculated as the intensity of the bound XATR relative to that of the pull-downed GST-XCDC6. The mean ± s.d. from three independent experiments are given with the control reaction with buffer alone set at 100% (lower panel). (C) Schematic of the experimental procedure for D, E and F. Sperm nuclei (2000/μl) were incubated in the egg extracts. After 15 minutes, human CDC6 fragments 180-220 or 1-180 with the SV40 T-antigen nuclear localization signal or buffer alone were added. (D,E) As indicated, aphidicolin (4 μg/ml) was also added to the reactions and, after a further 45-minute incubation, isolated nuclei (D) or chromatin (E) were immunoblotted with the indicated antibodies. The signal intensities of the phospho-Ser344 XChk1 (D) or XATR (E) bands induced by aphidicolin were quantified and normalized to those of whole XChk1 bands and XORC2 bands, respectively. The mean ± s.d. from three independent experiments are shown with the value for the control reaction with buffer alone set at 100% (each lower panel). (F) [^{32}P]-dCTP was added and, after a further 45-minute incubation, DNA replication was measured by [^{32}P] incorporation. The mean ± s.d. from three independent experiments are shown with the control reaction with buffer alone set at 100%.

Discussion

We have shown here that human CDC6 physically interacts with ATR in a Cdk-phosphorylation-stimulated manner (Figs 1, 2) and that CDC6 is required for the ATR-dependent replication-checkpoint response (i.e. inhibition of premature mitotic entry) activated by modest replication stress (Fig. 3). Interestingly, the defect in the checkpoint response caused by CDC6 depletion was rescued by the CDC6 EEE mutant mimicking Cdk phosphorylation, but not by the AAA mutant deficient in Cdk phosphorylation and ATR interaction (Fig. 4). Therefore, the CDC6 AAA mutant represents a mutant in which two functions of CDC6, replication licensing and replication-checkpoint regulation, are separated at the molecular level. In fission yeast, such mutant Cdc18 (CDC6) has not been identified yet. The region that we identified as an ATR-binding region on CDC6 does not include Cdk-phosphorylation sites (Fig. 1C). CDC6 is exported to the cytoplasm through Cdk phosphorylation but potential nuclear export signals on CDC6 are located at amino acids 462-488 (Delmolino et al., 2001), relatively distant from the Cdk-phosphorylation sites. However, it is conceivable that Cdk phosphorylation alters the high-order structure of CDC6 and thereby exposes the hidden nuclear export signals and ATR-binding region. In addition, the data reported here indicate that regulation of replication-checkpoint activation by CDC6-ATR interaction also occurs in *Xenopus* egg extracts: the XCDC6-XATR interaction was conserved (Fig. 5), and sequestration of the interaction by a human CDC6-derived peptide that binds to XATR reduced XATR chromatin recruitment and XChk1 phosphorylation induced by polymerase inhibition (Fig. 6).

These data, together with previously reported data in fission yeast (Hermand and Nurse, 2007), indicate that regulation of ATR-dependent replication-checkpoint activation through interaction between CDC6/CDC18 and ATR-ATRIP might be a conserved feature throughout eukaryotes. However, there are also differences among organisms. In the human cells studied here, this mechanism seems to play a crucial role for the replication checkpoint to be activated by modest replication stress, such as that elicited by 0.1 mM HU treatment (Fig. 3D,E, Fig. 4B), which reduces DNA synthesis by about half (Ge et al., 2007). Because CDC6 depletion alone (without additional replication perturbations) results in cells that prematurely enter mitosis with active DNA synthesis (Lau et al., 2006), the CDC6-ATR system might also operate against internal replication stress generated during the normal replication process. However, CDC6 in human cells seems dispensable for robust, ATR-dependent Chk1 phosphorylation induced by stronger replication stress, such as that induced by 2.5 mM HU treatment (Fig. 3C) (Lau et al., 2006). In addition, CDC6 is not required for ATR to accumulate at high levels in bright nuclear foci. CDC6 depletion somewhat affects ATR-dependent mitotic block activated by strong replication stress (i.e. 2.5 mM HU for 4 hours) but the relative contribution seems small (Fig. 3D,F).

A model that could reconcile these findings is depicted in Fig. 7. When replication stress is strong and, therefore, extensive RPA-coated ssDNA is generated, ATR-ATRIP molecules accumulate to high levels at the damaged sites through ATRIP-RPA interaction without the help of CDC6, forming bright ATR foci detectable by immunostaining, and robustly phosphorylate Chk1 (Fig. 7, left pathway). However, such high-level stable accumulation at damaged sites might be dispensable for ATR to be activated (Ball et al., 2005; Kim et al., 2005), although ATR foci formation could support some specific aspects of checkpoint responses. In other words, it is possible that only dynamic interaction between ATR and lesions is

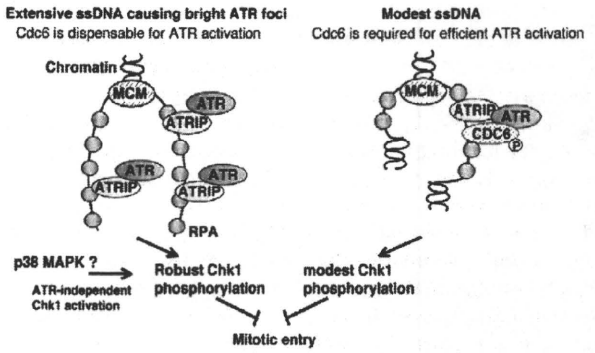

Fig. 7. Model for the role of human CDC6 in replication-checkpoint activation.

sufficient for ATR activation. In addition, in the presence of such extensive damage, another replication-checkpoint pathway(s) involving Chk1, but not ATR, could also be activated, leading to an ATR-independent (and thus caffeine-insensitive) block to mitosis (Rodríguez-Bravo et al., 2006). The p38 MAP kinase might be involved in such a pathway (Bulavin et al., 2001). Overall, CDC6 might have a minor role in checkpoint activation under such conditions.

However, even when cells are exposed to modest replication stress, ATR can be activated and delay mitotic entry despite low-level ATR foci formation and Chk1 phosphorylation (Fig. 3C,D). It is surprising that such low-level ATR activation can delay the cell cycle but, as in the *Xenopus* egg extract system, ATR is required to prevent premature mitotic entry not only when replication is inhibited by exogenous stress but also during normal DNA replication (Hekmat-Nejad et al., 2000). Presumably, fine regulatory control of the ATR-Chk1 pathway might function when cells encounter modest exogenous replication stress or endogenous replication stress. Under such circumstances, CDC6 and CDC6-ATR interaction might be required for ATR to elicit a mitotic block efficiently (Fig. 3D,E, Fig. 4B), presumably through regulating dynamic interaction between ATR and the damaged sites (Fig. 7, right pathway). Potential CDC6-RPA interactions could also play a role in this context. Extensive future studies will be required to clarify these points. Our present analyses of UV-damage-induced checkpoint responses found no indication of CDC6 involvement in these pathways. Although the details remain unclear, intermediates for checkpoint activation and subsequent signaling pathways might differ in some aspects between nucleotide-depletion-induced and UV-induced damage, as discussed above.

In contrast to human cells, in the *Xenopus* egg extract system, robust ATR-dependent Chk1 phosphorylation induced by 40 μM aphidicolin treatment seems dependent on XCDC6 (Oehlmann et al., 2004) and, as shown here, might be regulated by XCDC6-XATR interaction (Figs 5, 6). ATR chromatin recruitment induced by polymerase inhibition also depends on CDC6-ATR interaction in the *Xenopus* egg system (Fig. 6). The reason for the difference between the two systems, human cultured cells and *Xenopus* egg extracts, is not known at present. However, it should be emphasized that, even in the egg extract system, ORC-dependent, stable chromatin binding of XCDC6 is dispensable for XATR activation (Oehlmann et al., 2004), suggesting that the interactions between XCDC6 and the replication-checkpoint machinery are dynamic.

Journal of Cell Science

There is also a difference between human and fission yeast cells in terms of the CDC6-associated replication checkpoint. In yeast cells, Cdc18 (CDC6) is degraded during S phase depending on Cdk phosphorylation (Jallepalli et al., 1997; Jallepalli et al., 1998). Therefore, Cdc18 could not be involved in initial activation of the Rad3 (ATR)-dependent checkpoint. Attenuation of Cdk activity by the initial checkpoint activation then re-stabilizes Cdc18, which in turn interacts with Rad3-Rad26 (ATR-ATRIP) to sustain checkpoint activation (Hermand and Nurse, 2007). Therefore, these molecules seem to constitute a positive-feedback loop. However, in human cells, a significant part of CDC6 phosphorylated by Cdk remains in nuclei during S phase (Fujita et al., 1999) and CDC6 interaction with ATR is augmented by Cdk phosphorylation, as shown here (Fig. 2). Therefore, CDC6 might be involved in initial activation of an ATR-dependent checkpoint. When cells were treated with 0.1 mM HU for 4 hours, a condition under which we could definitely detect CDC6 involvement in replication-checkpoint activation, Cdk-phosphorylation-dependent CDC6 stabilization was not perturbed (Fig. 3C, Fig. 4A) and interaction of CDC6 with ATR was not affected (Fig. 2E). Therefore, ATR- and CDC6-dependent replication-checkpoint activation by modest replication stress might inhibit Cdk activity only to the extent that is insufficient for mitotic entry but enough for maintaining S-phase activity. If strong damage activates the replication checkpoint robustly and consequently inhibits Cdk activity markedly, then ATR-CDC6 interaction could be attenuated. However, under such conditions, CDC6 might be dispensable for checkpoint activation.

Materials and Methods

Cells

HeLa and 293T cells were grown in Dulbecco's modified Eagle's medium with 8% fetal calf serum. The chemicals used were: MG132 (Calbiochem), purvalanol A (Calbiochem), hydroxyurea (Sigma), caffeine (Nacalai) and aphidicolin (Sigma).

Expression of recombinant proteins and pulldown assay

GST-fusion proteins were bacterially produced and purified. GST pulldown assays were performed as described previously (Sugimoto et al., 2008), with 200 μg GST-fusion proteins per 2 ml extract from 1×10^8 cells. For pulldown assays with *Xenopus* egg extracts, 20 μl extracts were 40-fold diluted and then 6 μg GST-fusion proteins were added to the samples. Binding reactions for GST-fusion proteins were performed for 5 hours at 4°C. Human CDC6 fragments added to the *Xenopus* egg extracts were purified from the GST-fusion proteins by digestion with PreScission Protease (GE Healthcare).

Transfection and infection

293T cells were transfected as described previously (Sugimoto et al., 2008). HeLa cells were infected with retroviruses expressing the 2HA-CDC6 AAA mutant or EEE mutant, or with control retroviruses and selected with puromycin (0.5 μg/ml) as described (Sugimoto et al., 2008).

Immunoprecipitation and immunoblotting

Cells were extracted with modified CSK buffer containing 500 mM NaCl, 0.1% Triton X-100, 1 mM dithiothreitol (DTT) and multiple protease inhibitors (Sugimoto et al., 2008). Aliquots of the extracts were then immunoprecipitated with the indicated antibodies and protein-G–Sepharose beads (Amersham Bioscience). The beads were washed three times with NET gel buffer (Sugimoto et al., 2008). Immunoblotting and quantitation of the band signals were performed as described previously (Sugimoto et al., 2008).

siRNA experiments

siRNA oligonucleotides (IDT) were synthesized with the following sequences (sense strand): CDC6-1 (5′-AGACUAUAACUCUACAGAUUGUGdAdA-3′), CDC6-3 (5′-GGAGGACACUGGUUAAAGAAUUUdAdT-3′) and control scrambled (5′-CUUCCUCUCUUUCUCUCCCUUGUdGdA-3′). HeLa cells (4×10^4 cells per well in 12-well plates) were transfected with a 1:1 mixture of CDC6-1 and CDC6-3 or control siRNA duplexes (total 12 pmol; 6 nM) using HiPerFect transfection Reagent (Qiagen).

Immunostaining for phospho-histone H3

HeLa cells were washed, fixed with 3.7% formaldehyde, extracted with modified CSK buffer containing 0.1% Triton X-100, and then incubated overnight at 4°C with mouse anti-Ser10-phosphorylated histone H3 antibody. The samples were further incubated for 2 hours with Alexa-Fluor-594-conjugated goat anti-mouse IgG antibody (Molecular Probes), counterstained with DAPI and analyzed with a Leica FW4000 microscope.

Experiments with *Xenopus* egg extracts

Preparation of interphase egg extracts and de-membranated sperm nuclei, and the in vitro DNA-replication experiments were performed as described previously (Yoshida et al., 2005). Chromatin transfer experiments were performed as described previously (Hashimoto et al., 2006). Briefly, licensed sperm chromatin obtained after 15 minutes pre-incubation were diluted with ten volumes of EB buffer containing 0.1 mM NaCl and 2 mM DTT (Yoshida et al., 2005) and then centrifuged through a 20% sucrose layer at 10,000 ***g*** at 4°C for 5 minutes. The pellets were washed with EB containing 2 mM DTT and resuspended in second egg extracts. Immunodepletion of XCDC6 was carried out using 75 μl of anti-XCDC6 antisera for 100 μl egg extract (Yoshida et al., 2005). Nuclear and chromatin fractions were prepared as described previously (Kumagai et al., 1998; Yoshida et al., 2005). For immunoprecipitation, extracts were diluted with EB and then immunoprecipitated with the indicated antibodies and protein-G–Dynabeads (Invitrogen). The beads were washed three times with EB buffer containing 130 mM KCl.

Plasmids

For bacterial expression of GST-CDC6, pGEX6P-1-CDC6 was constructed by inserting human *CDC6* cDNA into pGEX6P-1 (GE Healthcare). *CDC6* truncated fragments were amplified by PCR using combinations of the following primers: 5′-1 primer, 5′-CGGGATCCGCTGTCGTCATGCCTCAAACCCG-3′; 5′-89 primer, 5′-CGGGATCCCATACACTTAAGGGACGAAGATTGG-3′; 5′-180 primer, 5′-CGGGATCCGATGTCATCAGGAATTTCTTGAGGG-3′; 3′-180 primer, 5′-TTA-AGCGGCCGCCTAATCCATCTCCCTTTCCCTGGC-3′; 3′-220 primer, 5′-TTAA-GCGGCCGCCTACTTGAGGTCTTGCAGAATCCG-3′; and 3′-268 primer, 5′-TTAAGCGGCCGCCTATTCCAATTTCCTCATCATGTCCTTC-3′. These PCR products were digested by *Bam*HI and *Not*I and subcloned into pGEX6P-1. For construction of fused SV40 T-antigen nuclear localization signal (NLS)-CDC6 fragments, an oligonucleotide containing the SV40 T-antigen NLS/*Bam*HI site/*Hin*dIII site sequence (5′-GATCGCCTAAAAAGAAGCGTAAAGTCGGATCCAAGCTTG-3′) and its complementary oligonucleotide were synthesized, annealed, inserted into the pGEX6P-1 *Bam*HI-*Eco*RI site, and CDC6 fragments were then introduced into the *Bam*HI-*Not*I site. pGEX6P-2-XCDC6 was provided by Haruhiko Takisawa (Osaka University, Osaka, Japan). Retrovirus vector pQCXIP-2HA-CDC6 was constructed by inserting *CDC6* cDNA tagged with tandem HA at its N-terminus into pQCXIP with a puromycin-resistance gene (Clontech). The cDNAs encoding Cdk-phosphorylation-deficient CDC6 AAA (Ser54, Ser74 and Ser106 were replaced with alanines) and phosphorylation-mimic EEE (Ser54, Ser74 and Ser106 were replaced with glutamates) mutants were gifts from Wei Jiang (Burnham Institute for Medical Research, La Jolla, CA). pBJ5.1-FLAG-ATR (Cliby et al., 1998) was kindly provided by Karlene Cimprich (Stanford University, Palo Alto, CA).

Antibodies

Preparation of antibodies against human CDC6, human MCM7, *Xenopus* ATR and *Xenopus* Chk1 were described previously (Hashimoto et al., 2006; Sugimoto et al., 2008). Antibodies against human Rad9, Hus1 and Rad1 were provided by Toshiki Tsurimoto (Kyushu University, Fukuoka, Japan). Other antibodies were purchased as follows: ATM (2C1, GeneTex), ATR (sc1887, Santa Cruz Biotechnology), ATRIP (number 2737, Cell Signaling), Cdh1 (c7855, Sigma), Chk1 (06-965, Upstate), Chk2 (05-649, Upstate), Claspin (ab3720, Abcam), cyclin A (sc596, Santa Cruz Biotechnology), Mre11 (611366, BD Bioscience), FLAG-M2 (F3165, Sigma Aldrich), Nbs1 (611870, BD Bioscience), Ser10-phosphorylated histone H3 (number 9706, Cell Signaling), Ser345-phosphorylated-Chk1 (number 2341 or 2348, Cell Signaling), Ser54-phosphorylated-CDC6 (sc12920R, Santa Cruz Biotechnology) and TopBP1 (ab2402, Abcam).

Statistical analysis

Statistical analysis was performed by a two-tailed Student's *t*-test to validate the data. *P*-values of <0.05 were considered statistically significant.

We thank Haruhiko Takisawa, Toshiki Tsurimoto, Wei Jiang, Koji Ode and Karlene Cimprich for Materials. We are also grateful to Satoko Yoshida, Chie Ogawa and Akiko Noguchi for assistance. This work was supported in part by a Grant to M.F. from the Ministry of Education, Culture, Sports, Science and Technology of Japan.

References

Ball, H. L., Myers, J. S. and Cortez, D. (2005). ATRIP binding to replication protein A-single-stranded DNA promotes ATR-ATRIP localization but is dispensable for Chk1 phosphorylation. *Mol. Biol. Cell* **16**, 2372-2381.

Bartek, J. and Lukas, J. (2003). Chk1 and Chk2 kinases in checkpoint control and cancer. *Cancer Cell* **3**, 421-429.

Bell, S. P. and Dutta, A. (2002). DNA replication in eukaryotic cells. *Annu. Rev. Biochem.* **71**, 333-374.

Brown, E. J. and Baltimore, D. (2003). Essential and dispensable roles of ATR in cell cycle arrest and genome maintenance. *Genes Dev.* **17**, 615-628.

Bulavin, D. V., Higashimoto, Y., Popoff, I. J., Gaarde, W. A., Basrur, V., Potapova, O., Appella, E. and Fornace, A. J., Jr (2001). Initiation of a G2/M checkpoint after ultraviolet radiation requires p38 kinase. *Nature* **411**, 102-107.

Burrows, A. E. and Elledge, S. J. (2008). How ATR turns on: TopBP1 goes on ATRIP with ATR. *Genes Dev.* **22**, 1416-1421.

Clay-Farrace, L., Pelizon, C., Santamaria, D., Pines, J. and Laskey, R. A. (2003). Human replication protein Cdc6 prevents mitosis through a checkpoint mechanism that implicates Chk1. *EMBO J.* **22**, 704-712.

Coleman, T. R., Carpenter, P. B. and Dunphy, W. G. (1996). The Xenopus Cdc6 protein is essential for the initiation of a single round of DNA replication in cell-free extracts. *Cell* **87**, 53-63.

Cortez, D., Guntuku, S., Qin, J. and Elledge, S. J. (2001). ATR and ATRIP: partners in checkpoint signaling. *Science* **294**, 1713-1716.

Cliby, W. A., Roberts, C. J., Cimprich, K. A., Stringer, C. M., Lamb, J. R., Schreiber, S. L. and Friend, S. H. (1998). Overexpression of a kinase-inactive ATR protein causes sensitivity to DNA-damaging agents and defects in cell cycle checkpoints. *EMBO J.* **17**, 159-169.

Delmolino, L. M., Saha, P. and Dutta, A. (2001). Multiple mechanisms regulate subcellular localization of human CDC6. *J. Biol. Chem.* **276**, 26947-26954.

Diffley, J. F. X. (2004). Regulation of early events in chromosome replication. *Curr. Biol.* **14**, R778-R786.

Drury, L. S., Perkins, G. and Diffley, J. F. X. (1997). The Cdc4/34/53 pathway targets Cdc6p for proteolysis in budding yeast. *EMBO J.* **16**, 5966-5976.

Duursma, A. and Agami, R. (2005). p53-dependent regulation of Cdc6 protein stability controls cellular proliferation. *Mol. Cell. Biol.* **25**, 6937-6947.

Feng, D., Tu, Z., Wu, W. and Liang, C. (2003). Inhibiting the expression of DNA replication-initiation proteins induces apoptosis in human cancer cells. *Cancer Res.* **63**, 7356-7364.

Fujita, M. (2006). Cdt1 revisited: complex and tight regulation during the cell cycle and consequences of deregulation in mammalian cells. *Cell Div.* **1**, 22.

Fujita, M., Yamada, C., Goto, H., Yokoyama, N., Kuzushima, K., Inagaki, M. and Tsurumi, T. (1999). Cell cycle regulation of human CDC6 protein. Intracellular localization, interaction with the human MCM complex, and CDC2 kinase-mediated hyperphosphorylation. *J. Biol. Chem.* **274**, 25927-25932.

Ge, X. Q., Jackson, D. A. and Blow, J. J. (2007). Dormant origins licensed by excess Mcm2-7 are required for human cells to survive replicative stress. *Genes Dev.* **21**, 3331-3341.

Gray, N. S., Wodicka, L., Thunnissen, A. M., Norman, T. C., Kwon, S., Espinoza, F. H., Morgan, D. O., Barnes, G., LeClerc, S., Meijer, L. et al. (1998). Exploiting chemical libraries, structure, and genomics in the search for kinase inhibitors. *Science* **281**, 533-538.

Guo, Z., Kumagai, A., Wang, S. X. and Dunphy, W. G. (2000). Requirement for Atr in phosphorylation of Chk1 and cell cycle regulation in response to DNA replication blocks and UV-damaged DNA in *Xenopus* egg extracts. *Genes Dev.* **14**, 2745-2756.

Hall, J. R., Kow, E., Nevis, K. R., Lu, C. K., Luce, K. S., Zhong, Q. and Cook, J. G. (2007). Cdc6 stability is regulated by the Huwe1 ubiquitin ligase after DNA damage. *Mol. Biol. Cell* **18**, 3340-3350.

Hashimoto, Y., Tsujimura, T., Sugino, A. and Takisawa, H. (2006). The phosphorylated C-terminal domain of *Xenopus* Cut5 directly mediates ATR-dependent activation of Chk1. *Genes Cells* **11**, 993-1007.

Hekmat-Nejad, M., You, Z., Yee, M. C., Newport, J. W. and Cimprich, K. A. (2000). *Xenopus* ATR is a replication-dependent chromatin-binding protein required for the DNA replication checkpoint. *Curr. Biol.* **10**, 1565-1573.

Herbig, U., Marlar, C. A. and Fanning, E. (1999). The Cdc6 nucleotide-binding site regulates its activity in DNA replication in human cells. *Mol. Biol. Cell* **10**, 2631-2645.

Hermand, D. and Nurse, P. (2007). Cdc18 enforces long-term maintenance of the S phase checkpoint by anchoring the Rad3-Rad26 complex to chromatin. *Mol. Cell* **26**, 553-563.

Jallepalli, P. V., Brown, G. W., Muzi-Falconi, M., Tien, D. and Kelly, T. J. (1997). Regulation of the replication initiator protein $p65^{cdc18}$ by CDK phosphorylation. *Genes Dev.* **11**, 2767-2779.

Jallepalli, P. V., Tien, D. and Kelly, T. J. (1998). sud1(+) targets cyclin-dependent kinase-phosphorylated Cdc18 and Rum1 proteins for degradation and stops unwanted diploidization in fission yeast. *Proc. Natl. Acad. Sci. USA* **95**, 8159-8164.

Jiang, W., Wells, N. J. and Hunter, T. (1999). Multistep regulation of DNA replication by Cdk phosphorylation of HsCdc6. *Proc. Natl. Acad. Sci. USA* **96**, 6193-6198.

Kan, Q., Jinno, S., Kobayashi, K., Yamamoto, H. and Okayama, H. (2008).Cdc6 determines utilization of $p21^{WAF1/CIP1}$-dependent damage checkpoint in S phase cells. *J. Biol. Chem.* **283**, 17864-17872.

Kastan, M. B. and Bartek, J. (2004). Cell-cycle checkpoints and cancer. *Nature* **432**, 316-323.

Kelly, T. J. and Brown, G. W. (2000). Regulation of chromosome replication. *Annu. Rev. Biochem.* **69**, 829-880.

Kim, S. M., Kumagai, A., Lee, J. and Dunphy, W. G. (2005). Phosphorylation of Chk1 by ATM- and Rad3-related (ATR) in *Xenopus* egg extracts requires binding of ATRIP to ATR but not the stable DNA-binding or coiled-coil domains of ATRIP. *J. Biol. Chem.* **280**, 38355-38364.

Kominami, K. and Toda, T. (1997). Fission yeast WD-repeat protein pop1 regulates genome ploidy through ubiquitin-proteasome-mediated degradation of the CDK inhibitor Rum1 and the S-phase initiator Cdc18. *Genes Dev.* **11**, 1548-1560.

Kumagai, A., Guo, Z., Emami, K. H., Wang, S. X. and Dunphy, W. G. (1998). The *Xenopus* Chk1 protein kinase mediates a caffeine-sensitive pathway of checkpoint control in cell-free extracts. *J. Cell Biol.* **142**, 1559-1569.

Kumagai, A., Lee, J., Yoo, H. Y. and Dunphy, W. G. (2006). TopBP1 activates the ATR-ATRIP complex. *Cell* **124**, 943-955.

Lau, E., Zhu, C., Abraham, R. T. and Jiang, W. (2006). The functional role of Cdc6 in S-G2/M in mammalian cells. *EMBO Rep.* **7**, 425-430.

Lau, E., Chiang, G. G., Abraham, R. T. and Jiang, W. (2009). Divergent S phase checkpoint activation arising from prereplicative complex deficiency controls cell survival. *Mol. Biol. Cell* **20**, 3953-3964.

Lee, J., Kumagai, A. and Dunphy, W. G. (2003). Claspin, a Chk1-regulatory protein, monitors DNA replication on chromatin independently of RPA, ATR, and Rad17. *Mol. Cell* **11**, 329-340.

Lee, J. H. and Paull, T. T. (2005). ATM activation by DNA double-strand breaks through the Mre11-Rad50-Nbs1 complex. *Science* **308**, 551-554.

Mailand, N. and Diffley, J. F. X. (2005). CDKs promote DNA replication origin licensing in human cells by protecting Cdc6 from APC/C-dependent proteolysis. *Cell* **122**, 915-926.

Méndez, J. and Stillman, B. (2000). Chromatin association of human origin recognition complex, Cdc6, and minichromosome maintenance proteins during the cell cycle: Assembly of prereplication complexes in late mitosis. *Mol. Cell. Biol.* **20**, 8602-8612.

Méndez, J., Zou-Yang, X. H., Kim, S. Y., Hidaka, M., Tansey, W. P. and Stillman, B. (2002). Human origin recognition complex large subunit is degraded by ubiquitin-mediated proteolysis after initiation of DNA replication. *Mol. Cell* **9**, 481-491.

Mordes, D. A., Glick, G. G., Zhao, R. and Cortez, D. (2008). TopBP1 activates ATR through ATRIP and a PIKK regulatory domain. *Genes Dev.* **22**, 1478-1489.

Namiki, Y. and Zou, L. (2006). ATRIP associates with replication protein A-coated ssDNA through multiple interactions. *Proc. Natl. Acad. Sci. USA* **103**, 580-585.

Nghiem, P., Park, P. K., Kim, Y., Vaziri, C. and Schreiber, S. L. (2001). ATR inhibition selectively sensitizes G1 checkpoint-deficient cells to lethal premature chromatin condensation. *Proc. Natl. Acad. Sci. USA* **98**, 9092-9097.

Nyberg, K. A., Michelson, R. J., Putnam, C. W. and Weinert, T. A. (2002). Toward maintaining the genome: DNA damage and replication checkpoints. *Annu. Rev. Genet.* **36**, 617-656.

Oehlmann, M., Score, A. J. and Blow, J. J. (2004). The role of Cdc6 in ensuring complete genome licensing and S phase checkpoint activation. *J. Cell Biol.* **165**, 181-190.

Pelizon, C., Madine, M. A., Romanowski, P. and Laskey, R. A. (2000). Unphosphorylatable mutants of Cdc6 disrupts its nuclear export but still support DNA replication once per cell cycle. *Genes Dev.* **14**, 2526-2533.

Petersen, B. O., Lukas, J., Sørensen, C. S., Bartek, J. and Helin, K. (1999). Phosphorylation of mammalian CDC6 by cyclin A/CDK2 regulates its subcellular localization. *EMBO J.* **18**, 396-410.

Rodríguez-Bravo, V., Guaita-Esteruelas, S., Florensa, R., Bachs, O. and Agell, N. (2006). Chk1- and claspin-dependent but ATR/ATM- and Rad17-independent DNA replication checkpoint response in HeLa cells. *Cancer Res.* **66**, 8672-8679.

Saha, P., Chen, J., Thome, K. C., Lawlis, S. J., Hou, Z. H., Hendricks, M., Parvin, J. D. and Dutta, A. (1998). Human CDC6/Cdc18 associates with Orc1 and cyclin-cdk and is selectively eliminated from the nucleus at the onset of S phase. *Mol. Cell. Biol.* **18**, 2758-2767.

Sugimoto, N., Kitabayashi, I., Osano, S., Tatsumi, Y., Yugawa, T., Narisawa-Saito, M., Matsukage, A., Kiyono, T. and Fujita, M. (2008). Identification of novel human Cdt1-binding proteins by a proteomics approach: proteolytic regulation by APC/C^{Cdh1}. *Mol. Biol. Cell* **19**, 1007-1021.

Sugimoto, N., Yoshida, K., Tatsumi, Y., Yugawa, T., Narisawa-Saito, M., Waga, S., Kiyono, T. and Fujita, M. (2009). Redundant and differential regulation of multiple licensing factors ensures prevention of re-replication in normal human cells. *J. Cell Sci.* **122**,1184-1191.

Villerbu, N., Gaben, A. M., Redeuilh, G. and Mester, J. (2002). Cellular effects of purvalanol A: a specific inhibitor of cyclin-dependent kinase activities. *Int. J. Cancer* **97**, 761-769.

Williams, R. S., Shohet, R. V. and Stillman, B. (1997). A human protein related to yeast Cdc6p. *Proc. Natl. Acad. Sci. USA* **94**, 142-147.

Yoshida, K., Takisawa, H. and Kubota, Y. (2005). Intrinsic nuclear import activity of geminin is essential to prevent re-initiation of DNA replication in Xenopus eggs. *Genes Cells* **10**, 63-73.

Zachos, G., Rainey, M. D. and Gillespie, D. A. (2003). Chk1-deficient tumour cells are viable but exhibit multiple checkpoint and survival defects. *EMBO J.* **22**, 713-723.

Zachos, G., Rainey, M. D. and Gillespie, D. A. (2005). Chk1-dependent S-M checkpoint delay in vertebrate cells is linked to maintenance of viable replication structures. *Mol. Cell. Biol.* **25**, 563-574.

Zhao, H. and Piwnica-Worms, H. (2001). ATR-mediated checkpoint pathways regulate phosphorylation and activation of human Chk1. *Mol. Cell. Biol.* **21**, 4129-4139.

Zou, L. and Elledge, S. J. (2003). Sensing DNA damage through ATRIP recognition of RPA-ssDNA complexes. *Science* **300**, 1542-1548.

Journal of Cell Science

Virus Genes
DOI 10.1007/s11262-009-0447-x

The PDZ domain binding motif (PBM) of human T-cell leukemia virus type 1 Tax can be substituted by heterologous PBMs from viral oncoproteins during T-cell transformation

Tomoya Aoyagi · Masahiko Takahashi · Masaya Higuchi · Masayasu Oie · Yuetsu Tanaka · Tohru Kiyono · Yutaka Aoyagi · Masahiro Fujii

Received: 28 July 2009 / Accepted: 30 December 2009
© Springer Science+Business Media, LLC 2010

Abstract Several tumor viruses, such as human T-cell leukemia virus (HTLV), human papilloma virus (HPV), human adenovirus, have high-oncogenic and low-oncogenic subtypes, and such subtype-specific oncogenesis is associated with the PDZ-domain binding motif (PBM) in their transforming proteins. HTLV-1, the causative agent of adult T-cell leukemia, encodes Tax1 with PBM as a transforming protein. The Tax1 PBM was substituted with those from other oncoviruses, and the transforming activity was examined. Tax1 mutants with PBM from either HPV-16 E6 or adenovirus type 9 E4ORF1 are fully active in the transformation of a mouse T-cell line from interleukin-2-dependent growth into independent growth. Interestingly, one such Tax1 PBM mutant had an extra amino acid insertion derived from E6 between PBM and the rest of Tax1, thus suggesting that the amino acid sequences of the peptides between PBM and the rest of Tax1 and the numbers only slightly affect the function of PBM in the transformation. Tax1 and Tax1 PBM mutants interacted with tumor suppressors Dlg1 and Scribble with PDZ-domains. Unlike E6, Tax1 PBM mutants as well as Tax1 did not or minimally induced the degradations of Dlg1 and Scribble, but instead induced their subcellular translocation from the detergent-soluble fraction into the insoluble fraction, thus suggesting that the inactivation mechanism of these tumor suppressor proteins is distinct. The present results suggest that PBMs of high-risk oncoviruses have a common function(s) required for these three tumor viruses to transform cells, which is likely associated with the subtype-specific oncogenesis of these tumor viruses.

Keywords HTLV-1 · Tax · PDZ · PBM

Tomoya Aoyagi and Masahiko Takahashi contributed equally to this study.

T. Aoyagi · M. Takahashi · M. Higuchi · M. Oie · M. Fujii (✉)
Division of Virology, Graduate School of Medical and Dental Sciences, Niigata University, 1-757 Asahimachi-Dori, Niigata 951-8510, Japan
e-mail: fujiimas@med.niigata-u.ac.jp

T. Aoyagi · Y. Aoyagi
Division of Gastroenterology and Hepatology, Graduate School of Medical and Dental Sciences, Niigata University, 1-757 Asahimachi-Dori, Niigata 951-8510, Japan

Y. Tanaka
Department of Immunology, Graduate School and Faculty of Medicine, University of the Ryukyus, Okinawa, Japan

T. Kiyono
Virology Division, National Cancer Center Research Institute, Chuo-ku, Tokyo, Japan

Introduction

Human T-cell leukemia virus (HTLV) has two subtypes with distinct pathogenicities [1–3]. The type 1 virus (HTLV-1) is the etiologic agent of adult T-cell leukemia, whereas type 2 one (HTLV-2) is not associated with any malignancies. These two viruses immortalize human T-cells in vitro with equivalent efficiency. Therefore, the distinct pathogenicities are likely to be in the later step of the leukemogenesis [4]. Accumulating evidence suggests the crucial involvement of HTLV-1 Tax1 protein in the aggressive pathogenicity of HTLV-1 relative to HTLV-2 [5–8].

Tax1 and Tax2 are the transforming proteins of HTLV-1 and HTLV-2, respectively, which are essential for the viruses to immortalize human T-cells in vitro [7, 9–12]. Tax1 and Tax2 have multiple activities such as transcriptional activation of cellular genes through NF-κB, CREB/

Published online: 13 January 2010

ATF, SRF and AP-1 and the inactivation of tumor suppressor proteins p53 and p16INK4a [13–18], but they are generally equivalent to each other. Tax1 and Tax2 have, however, a significant difference in the transforming activities in vitro [5, 6]. For instance, Tax1 transforms a mouse T-cell line CTLL-2 from interleukin (IL)-2-dependent growth into independent growth, and the activity was much greater than that of Tax2 [6]. Subsequent studies identified two Tax1-specific activities responsible for the distinct transforming activities. One is the activity through the PDZ domain binding motif (PBM) present only in Tax1 but not in Tax2 [6, 19], and the other is the activation of transcription factor NF-κB2 [8]. Therefore, elucidating these differences would uncover the molecular mechanism underlying the distinct pathogenicities of these viruses.

Human papilloma virus (HPV) and human adenovirus are associated with human cervical cancer and estrogen-dependent mammary tumors in female rats, respectively. Interestingly, they also have high-oncogenic subtypes and low-oncogenic ones, and only the high-oncogenic subtypes have PBM in the transforming proteins such as E6 of HPV type 16 and E4ORF1 of adenovirus type 9 [20, 21]. Tax1 PBM mutants were produced either with HPV-16 E6 or E4ORF1 of adenovirus type 9 to examine whether these PBM are functionally substitutable in the functions. These heterologous PBMs from other high-pathogenic oncoviruses fully substituted for Tax1 PBM in the transformation. These results further supported the hypothesis that PBMs of viral oncoproteins have a common function in the transformation, and thus also in the subtype-specific oncogenesis of tumor viruses.

Materials and methods

Cells and culture conditions

293T cells are derived from the human embryonic kidney. This cell line was cultured in Dulbecco's modified Eagle's medium (DMEM) supplemented with 10% heat inactivated fetal bovine serum (FBS), 4 mM L-glutamine, penicillin (50 U/ml), and streptomycin (50 μg/ml) at 37°C in 5% CO_2. Human T-cell lines used in the present experiments have been characterized previously [19, 22]. Jurkat and MOLT-4 are HTLV-1-negative T-cell lines. MT-4 and SLB-1 are HTLV-1-infected human T-cell lines. These T-cell lines were cultured in RPMI1640 supplemented with 10% FBS, 4 mM L-glutamine, penicillin (50 U/ml), and streptomycin (50 μg/ml; RPMI/10%FBS). CTLL-2 is a mouse T lymphocyte cell line which was cultured in RPMI/10%FBS supplemented with 55 μM 2-mercaptoethanol and 500 pM recombinant human IL-2 (RPMI/10%FBS/IL-2) at 37°C in 5% CO_2.

Plasmids

The lentiviral vector CSII-EF-IG-RfA and the expression vector pHβPr-1-neo were used for the expression of Tax1 or its mutant proteins, as previously described [5, 8]. Tax1ΔC is a PBM-negative mutant and has four amino acid deletion from the C-terminus of Tax1 [19]. M1, M2, and M3 are Tax1 PBM mutants and have PBM from adenovirus type 9 E4ORF1 (ATLV), HPV-16 E6 (ETQL), and HPV-16 E6 (RSSRTRRETQL), respectively. The mutations were introduced using the polymerase chain reaction (PCR). The 3′-primers used for PCR were 5′-TC AGACAAGTGTAGCTCGGAAATGTTTTTCACT-3′ for M1, 5′-TCAAAGTTGTGTTTCTCGGAAATGTTTTTCA CT-3′ for M2, and 5′-TCAAAGTTGTGTTTCGCGGCGT GTGCGGCTGCTGCGTCGGAAATGTTTTTCACT For M3. The common 5′-primer was 5′-AACAGCTATGAC-CATG-3′ corresponding to the pBluescript-tax1 plasmid, which has the wild-type tax1 gene. After the mutations were confirmed by DNA sequencing, these genes were cloned into pENTR/D-TOPO (Invitrogen) and then were transferred to CSII-EF-IG-RfA by an LR recombination reaction using LR clonase (Invitrogen). In addition, the tax1 mutant genes were cloned into pHβPr-1-neo plasmid.

Cell lysate preparation

The 293T and human T-cell lines were treated with lysis buffer [1% NP40, 25 mM Tris–HCl (pH 7.2), 150 mM NaCl, 1 mM EDTA, 1 mM phenylmethylsulfonyl fluoride and 2 μg/ml leupeptin] at 4°C for 15 min to prepare detergent soluble and insoluble fractions. After centrifugation, the supernatant was collected and used as a soluble fraction, and the resultant pellet was suspended in sodium dodecyl sulfate (SDS) sample buffer [2% SDS, 62.5 mM Tris–HCl (pH 6.8), 20% glycerol, 0.01% bromophenol blue, 50 mM dithiothreitol], and then heated at 95°C for 5 min. After centrifugation, the supernatants were used as the insoluble fraction. To prepare total lysates, the cells were suspended with the SDS sample buffer and heated at 95°C for 5 min. After centrifugation, the supernatants were used as the total cell lysates.

Western blotting

Soluble fraction (30 μg), insoluble fraction (20 μg), and total cell lysates (20 μg) were size-separated on 6–12% polyacrylamide gel containing SDS and then were electronically transferred to the PVDF membranes. The membranes were incubated with the primary antibody, followed by the corresponding secondary antibody labeled with peroxidase, and then were visualized using an ECL Western blotting detection system (GE Healthcare). The

primary antibodies used were anti-Tax1 monoclonal antibody (TAXY-7) [23], anti-HA (HA-7 from Sigma), anti-Scribble (K-21, Santa Cruz Biotechnology, Santa Cruz, CA), mouse anti-Dlg1 monoclonal antibody (BD Biosciences Pharmingen, San Diego, CA), mouse anti-α-Tubulin monoclonal antibody (Calbiochem), and goat anti-Lamin B polyclonal antibody (Santa Cruz).

Co-immunoprecipitation assay

The co-immunoprecipitation assay was performed as described previously [24]. Briefly, the pHβPr-1-Tax1 or its mutant plasmids were transiently transfected into 293T cells by lipofection (Fugene6, Roche Molecular Systems, Peasanton, CA). Forty-eight hours after the transfection, the cells were treated with lysis buffer supplemented with 1 mM phenylmethylsulfonyl fluoride and 2 μg/ml leupeptin, and the lysates were cleared by centrifugation and immunoprecipitated with anti-Tax1 antibody (TAXY-7). The immunoprecipitated proteins were analyzed by Western blotting using anti-Scribble (K-21, Santa Cruz Biotechnology), anti-Dlg1 monoclonal antibody (BD Biosciences Pharmingen), and anti-Tax1, respectively. The antibody binding to the membrane was visualized using an ECL Western blotting detection system (GE Healthcare).

Transformation assay

Recombinant lentiviruses were generated by transfecting pCAG-HIVgp, pCMV-VSV-G-RSV-Rev (provided by H. Miyoshi) and the respective lentiviral vector plasmids (Tax1, Tax1ΔC, M1, M2, M3 in CSII-EF-IG-RfA) into 293T cells by using FuGENE6 (Roche). The supernatant containing the respective viruses was then infected into the CTLL-2 cells (5×10^5) in 2 ml of RPMI/10%FBS/IL-2 medium containing 8 μg/ml polybrene (Sigma). Forty-eight hours after infection, the cells were washed four times with phosphate-buffered saline (PBS), suspended in RPMI/10%FBS without IL-2, and cultured in a 96-well plate (3,000 cells/well, 5,000 cells/well, 10,000 cells/well) for 3 weeks. During the culture period, the medium was changed every three days. Next, the number of wells containing outgrowing cells was counted using a light microscope. The transformation (number) was then determined based on the number of positive wells out of 96 wells.

Immunostaining analysis

To analyze the subcellular localization of Tax1, Tax1 PBM mutants, Dlg1 and Scribble proteins in 293T cells, the cells were cultured on glass slides in 6-well culture plate overnight, and then the cells were transiently transfected with either the pHβPr-neo-Tax1, pHβPr-neo-Tax1ΔC, pHβPr-neo-Tax1M1, pHβPr-neo-Tax1M2 or pHβPr-neo-Tax1M3 plasmid using the lipofection method (FuGENE 6). At 48 h after transfection, the cells were fixed with 4% formaldehyde in PBS for 25 min at 4°C. The fixed cells were then incubated with the mouse anti-Dlg1 antibody (BD Biosciences Pharmingen) and the serum from an HTLV-1 carrier for Dlg1 analysis, or incubated with the rabbit anti-Scribble antibody (H-300) and the mouse anti-Tax1 antibody (TAXY-7) for a Scribble analysis. After washing, the cells were incubated with Alexa 594 labeled anti-mouse IgG (Molecular Probes, Eugene, OR) and fluorescein isothiocyanate labeled anti-human IgG (Beckman Coulter, Fullerton, CA) for Dlg1 analysis, or incubated with Alexa 594 labeled anti-mouse IgG (Molecular Probes) and Alexa 488 labeled anti-rabbit IgG (Molecular Probes) for a Scribble analysis. After washing, the cells were stained with Hoechst 33258. The stained cells were then examined by fluorescent microscopy (BZ-8000, KEYENCE).

Results

Functional substitution of Tax1 PBM by heterologous PBMs

Three Tax1 PBM mutants were produced to examine whether PBMs of other oncoproteins can substitute Tax1 PBM in the transformation. M1 and M2 have the PBM of adenovirus type 9 E4ORF1and HPV-16 E6 (ATLV and ETQL instead of ETEV in Fig. 1a), respectively. M3 has the 11 amino acid from the E6 C-terminus including PBM and thus have an extra seven amino acid residues relative to Tax1. The lentiviruses encoding these Tax1 mutants as well as Tax1ΔC without Tax1 PBM were cultured with an IL-2-dependent T-cell line (CTLL-2) for 24 h, and then cultured without IL-2 for 3 weeks on 96-well plates. The wells with outgrowing cells were counted by a light microscope. Cells infected with the control lentivirus or with lentivirus encoding Tax1ΔC without PBM did not induce the outgrowth of CTLL-2 cells (Fig. 1b). On the other hand, all three Tax1 PBM mutants efficiently induced the outgrowth, although the activities were not as strong as those of wild type Tax1. The inability of Tax1ΔC to transform CTLL-2 was not due to the quantity of the Tax1ΔC proteins in CTLL-2, since a Western blotting analysis detected the equivalent amount of Tax1ΔC protein to those of Tax1 in CTLL-2 (Fig. 1c). It should be noted that a substitution mutation of Tax1 amino acid 353 from Val to Ala (Tax353A) or 351 from Thr to Ala (Tax351A) abrogated the transforming activity [6], denying that the addition of any four amino acids to Tax1 C-terminus can rescue the transforming activity. Therefore, these results

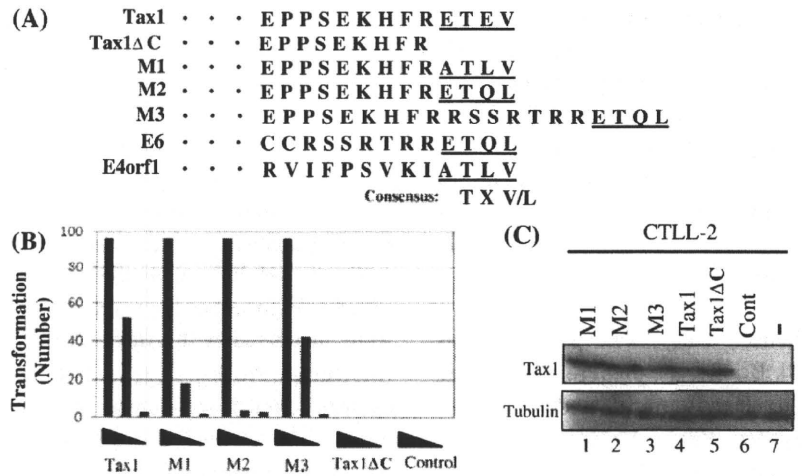

Fig. 1 The functional substitution of Tax1 PBM by heterologous PBMs of viral oncoproteins. **a** Amino acid sequences of the C-terminal ends of three oncoproteins and Tax1 mutants. **b** The cell lysates were prepared from CTLL-2 cells infected with lentiviruses encoding the indicated Tax1 mutants or the control lentivirus (Cont), and they were characterized by a Western blotting analysis using anti-Tax1 antibody. **c** CTLL-2 cells were infected with lentiviruses encoding Tax1 or the indicated Tax1 mutants, or the control lentivirus (Cont). They were cultured with IL-2 for 24 h, washing with PBS, and then cultured without IL-2 for 3 weeks on 96-well plate in the density of 1,000 cells/well, 3,000 cells/well or 10,000 cells/well. The wells containing outgrowing cells were counted by a light microscope. The transformation (number) is the number of wells containing outgrowing cells (the maximum number is 96)

indicated that the PBM from two oncoviruses can substitute for the function of the Tax1 PBM in the transformation. Unlike other PBM mutants, M3 has extra amino acid residues in front of PBM derived from E6 (Fig. 1a), thus indicating that PBM can flexibly perform its function(s) in the transformation.

Tax1 mutants interact with PDZ domain proteins

Tax1 is known to interact with multiple PDZ domain proteins including Dlg1 and Scribble [24–26], and the interactions are strongly correlated with the transforming activity toward CTLL-2 [22]. Tax1 expression plasmids were transfected into 293T cells. The lysates prepared from the transfected cells were then immunoprecipitated with anti-Tax1 antibody, and the proteins precipitated with Tax1 were characterized with anti-Dlg1 or anti-Scribble antibody. Anti-Tax1 antibody co-immunoprecipitated endogenous Dlg1 and Scribble together with wild type Tax1 or its PBM mutants (M1, M2, M3), but not with Tax1ΔC, thus indicating that Dlg1 and Scribble interact with Tax1 mutants in a heterologous PBM-dependent manner (Fig. 2). In addition, the amount of Dlg1 and Scribble in soluble cell lysates was reduced by the interaction with Tax1 and its mutant. A previous study showed that Dlg1 is translocated to the detergent insoluble fraction through binding to Tax1 [19]. Three cell lysates (namely, the detergent soluble fraction, the detergent insoluble fraction, the total lysate) were prepared from the 293T cells transfected with the Tax1 plasmids used above to examine whether Tax1 has similar activity to Scribble. While Tax1 or its mutants interacting with these PDZ domain proteins

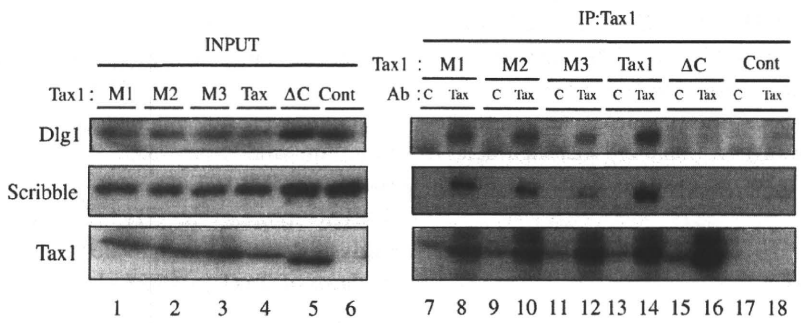

Fig. 2 Tax1 PBM mutants can interact with Dlg1 and Scribble. Cell lysates were prepared from 293T cells transfected with the expression plasmids encoding the indicated Tax1 mutants or the control plasmid (*Cont*). An aliquot of the lysates were immunoprecipitated with anti-Tax1 antibody (*Tax*) or the control antibody (*C*). The total cell lysates (*Input*) and immunoprecipitates (*IP*) were characterized by a Western blot analysis using anti-Dlg1, anti-Scribble, or anti-Tax1 antibody